


5-2014

Impacts of Carbonate Mineral Weathering on Hydrochemistry of the Upper Green River Basin, Kentucky

Laura Leigh Osterhoudt
Western Kentucky University, losterhoudt@hotmail.com

Follow this and additional works at: <http://digitalcommons.wku.edu/theses>

 Part of the [Geochemistry Commons](#), [Hydrology Commons](#), and the [Physical and Environmental Geography Commons](#)

Recommended Citation

Osterhoudt, Laura Leigh, "Impacts of Carbonate Mineral Weathering on Hydrochemistry of the Upper Green River Basin, Kentucky" (2014). *Masters Theses & Specialist Projects*. Paper 1337.
<http://digitalcommons.wku.edu/theses/1337>

This Thesis is brought to you for free and open access by TopSCHOLAR®. It has been accepted for inclusion in Masters Theses & Specialist Projects by an authorized administrator of TopSCHOLAR®. For more information, please contact connie.foster@wku.edu.

IMPACTS OF CARBONATE MINERAL WEATHERING
ON HYDROCHEMISTRY OF THE
UPPER GREEN RIVER BASIN, KENTUCKY

A Thesis
Presented to
The Faculty of the Department of Geography and Geology
Western Kentucky University
Bowling Green, Kentucky

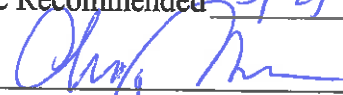
In Partial Fulfillment
of the Requirements for the Degree
Master of Science

By
Laura Leigh Osterhoudt

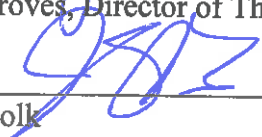
May 2014

IMPACTS OF CARBONATE MINERAL WEATHERING
ON HYDROCHEMISTRY OF THE
UPPER GREEN RIVER BASIN, KENTUCKY

Date Recommended 5/2/14



Chris Groves, Director of Thesis



Jason Polk



Fred Siewers



Dean, Graduate School

5-6-14

Date

ACKNOWLEDGMENTS

I would like to acknowledge those individuals and institutions that have been instrumental in the completion of this Master's thesis. Dr. Chris Groves has been exceptionally influential in my growth both as a student and a person. I will forever be grateful for his wisdom and friendship. I would also like to thank my committee members for their contributory roles in the discussions, implementation, and ultimately the completion of this research. I am also appreciative of the work Kegan McClanahan has contributed to this project, both in discussions and in the field. WKU's Applied Research and Technology Program provided the principal funding for the project. The Center for Biodiversity Studies and the Western Kentucky Green River Preserve provided equipment and land, which proved to be instrumental for this research. I would also like to thank Dr. Ouida Meier, Dr. Albert Meier and Dr. Scott Grubbs for the use of their equipment and thoughtful discussions. In addition, words cannot express the gratitude I have for the family and friends who have supported me throughout my academic career. My husband and children have been there for me every step of the way through both my undergraduate and graduate careers and have made exemplary efforts to support me with all my goals. My mom has also made it possible for me to complete my degree through all her support and I will forever be grateful.

CONTENTS

Abstract	Error! Bookmark not defined.
Chapter 1: Introduction	1
Literature Review	3
Carbon Cycle	3
Karst	9
Geochemistry	16
Carbon Sequestration in Karst	18
Chapter 2: Study Area	21
Background	22
Chapter 3: Methodology	27
Site Selection	27
Site Installation	31
Mapping Methods	33
Sample Collection	37
Laboratory Analysis	42
Data Analysis	456
DIC and Carbon Flux	50
Chapter 4: Results and Conclusion	53
Results of pH Data	53
Results of SpC Data	57
Results of Water Temperature Data	59
Results for Discharge Data	62
Relationships in Hydrochemistry	63
Ionic Relationship	66
Dissolved Inorganic Carbon	Error! Bookmark not defined.
Conclusion	Error! Bookmark not defined.0
References	76

LIST OF FIGURES

Figure 1- Karst in the Upper Green River basin. Source of karst data: Currens et al. (2002).	11
Figure 2- Springs Located Within Nested Watersheds of Upper Green River Basin. Source of spring data KGS (2013).	13
Figure 3- Sinkholes Located Within Watersheds of Upper Green River Basin. Source of sinkhole data KGS (2013).	14
Figure 4- Map of Watershed Lithology. Source of lithology data KGS (2013).	23
Figure 5- Stratigraphy of Region, Source: Kentucky Geological Survey (1939).	25
Figure 6- Greensburg, USGS gaging station, (A) grab sample site (B) data logger site.	28
Figure 7- (A) Munfordville data logger site, (B) PVC encasements for data loggers.	28
Figure 8- Greensburg field site.	30
Figure 9- Munfordville field site.	31
Figure 10- Upper Green River Study Area Basin Boundaries.	34
Figure 11- Basin Boundary Comparison, Munfordville.	35
Figure 12- Hold time for anions (Jackson 2000).	43
Figure 13- Average of Orange and Blue pH probes, Greensburg field site.	47
Figure 14- Continuous SpC from two Greensburg sondes with grab sample SpC data.	478
Figure 15- Rating Curve used for Greensburg Discharge.	50
Figure 16- Graph of pH values for Greensburg and Munfordville.	54
Figure 17- Graphs of warm and cold period pH variations, Greensburg and Munfordville, KY. .	56
Figure 18- Difference in watershed pH, Munfordville – Greensburg.	57
Figure 19- Graph of SpC for Greensburg and Munfordville.	58
Figure 20- Ratio of Munfordville and Greensburg specific conductance.	59
Figure 21- Graph of Temperature vs. Julian Date after October 21, 2013.	60
Figure 22- Graph of Temperature vs. Julian Date after October 21, 2013.	61
Figure 23- Difference in field site water temperature.	61
Figure 24- Graph of Discharge l/s for field sites.	62
Figure 25- Graph of SpC and Discharge, Greensburg.	64
Figure 26- Graph of SpC and Discharge, Munfordville.	64
Figure 27- Graph of pH and SpC, Greensburg.	65
Figure 28- Graph pH and SpC, Munfordville.	65
Figure 29- HCO ₃ ⁻ and SpC, Greensburg.	67
Figure 30- HCO ₃ ⁻ and SpC, Munfordville.	67
Figure 31- Ca ²⁺ vs SpC, Greensburg.	67
Figure 32- Ca ²⁺ vs SpC, Munfordville.	67
Figure 33- Mg ²⁺ vs SpC, Greensburg.	68
Figure 34- Mg ²⁺ vs SpC, Munfordville.	688
Figure 35- Table of differences in 15-minute resolution data.	69
Figure 36- Atmospheric carbon flux and DIC results for Greensburg and Munfordville watersheds.	70

IMPACTS OF CARBONATE MINERAL WEATHERING
ON THE HYDROCHEMISTRY OF THE
UPPER GREEN RIVER BASIN, KENTUCKY

Laura Leigh Osterhoudt

May 2014

Pages 81

Directed by: Dr. Chris Groves, Dr. Jason Polk, and Dr. Fred Siewers

Department of Geography and Geology

Western Kentucky University

Kentucky's Upper Green River Basin has received significant attention due to the area's high biodiversity and spectacular karst development. While carbonate bedrock is present throughout the watershed, it is more extensive and homogenous along the river between Greensburg and Munfordville than upstream from Greensburg where the geology is more heterogeneous. This research quantitatively evaluated how lithological differences between the two catchment areas impact hydrochemistry and inorganic carbon cycling. This first required correcting catchment boundaries on previous US Geological Survey Hydrologic Unit Maps to account for areas where the boundaries cross sinkhole plains. Basin boundaries using existing Kentucky Division of Water dye trace data differed from the earlier versions by as much as three kilometers.

The river at the downstream site is more strongly influenced by carbonate mineral dissolution, reflected in higher specific conductance (SpC) and pH. The SpC at Munfordville ranges from 0.9 to 4.8 times that at Greensburg, averaging 2.0 times higher. Although rainfall is impacted by sulfuric acid from coal burning, river pH is buffered at both sites. The pH is higher at Munfordville 91% of the time, by an average of 0.28 units. Diurnal, photosynthetic pH variations are damped out downstream suggesting interactions between geologic and biological influences on river chemistry. River temperature differences between the two sites are at least 4°C higher at Greensburg under warm season

conditions, but there is a clear trend of temperature differences diminishing as the river cools through the fall and winter. This results from a relatively stable temperature at Munfordville, impacted by large spring inputs of groundwater within the karst region downstream. Although weak statistical relationships between SpC and HCO_3^- create uncertainties in high resolution carbon flux calculations, measurement of these fluxes is more highly impacted by discharge variations than concentration variations, which resulted in average daily atmospheric flux estimates within 34% between the two basins using weekly concentration data (3.3×10^8 vs. 2.2×10^8 $\text{gkm}^{-2} \text{d}^{-1}$, where km^2 is the outcrop area of carbonate rocks), and within only 12% using 15-minute concentration data from regressions (2.6×10^8 vs. 2.3×10^8 $\text{gkm}^{-2} \text{d}^{-1}$) for Greensburg and Munfordville, respectively.

Chapter 1: Introduction

The global carbon budget fluctuates primarily through a series of exchanges between the atmosphere, the ocean and associated sediments, terrestrial rocks, and vegetation. Within each of these interactions are many detailed processes that involve physical, geochemical, and biological transformations. Fluvial systems transport carbon dioxide (CO₂) to the world's oceans, and a large amount of the CO₂ in these systems derives from atmospheric sources (Meybeck 1983; Sarmiento and Sundquist 1992; Amiotte-Suchet and Probst 1995; Amiotte-Suchet et al. 2003). These elements all come together to create the carbon cycle, and a full quantification of this has proven difficult due to the large number, and complexity, of exchanges within the system. Each environment provides for different carbon exchanges depending upon many variables, which include the lithology, climate, and vegetation. For these purposes, site-specific research is pertinent to better understand inferences with respect to relationships between specific local processes and the overall global carbon budget.

The Green River, a tributary of the Ohio River, flows westward through south-central Kentucky over heterogeneous, Paleozoic sedimentary rocks, dominated in some reaches by karstic carbonate bedrock. The section of river west and downstream from the Green River Reservoir Dam near Munfordville is extraordinarily biodiverse (Master et al. 1998) providing an excellent study area for carbon interactions between the atmosphere, the river and its related flow systems, carbonate rock, and aquatic vegetation. This research focuses on inorganic carbon dynamics within two nested watersheds of the upper Green River, including the areas draining to Greensburg and Munfordville, KY, respectively. Munfordville is approximately 50 km downstream from Greensburg. The Green River

upstream from Munfordville flows over carbonate rock through much of its journey, though upstream from field site 1 (Greensburg), the geology tends to be heterogeneous, with interbedded, clastic rocks and relatively impure limestones, while downstream from site 2 (Munfordville) the carbonate rock outcrops are continuous, increasingly pure, and create a globally significant karst landscape (Dicken 1935; White and White 1989). Due to the potentially significant contribution of carbonate rock weathering as a potential carbon sink on the continents, which is estimated at 6.1×10^7 gigatons per year (Gt/yr) (Ludwig et al. 1999; Liu and Zao 2000), investigating the inorganic carbon fluctuations along this reach of the Upper Green River provides insight into quantifying landscape-atmosphere carbon interactions within fluvial/karst carbonate karst environments.

This research provides a hydrochemical analysis of the inorganic carbon dynamics of the Upper Green River through a comparison between two contributing watersheds to better understand the carbon budget in this type of hydrogeological environment. This study addressed the following research questions:

1. What are the magnitude of the atmospheric carbon sink from carbonate mineral weathering in the Greensburg and Munfordville watersheds?
2. How do differences in lithology and hydrogeology between the two basins impact river hydrochemistry?
3. High-resolution methods exploiting significant linear statistical relationships between specific conductance (SpC) and calcium (Ca^{2+}) and SpC and bicarbonate (HCO_3^-) ions have been used to measure such carbon sinks in homogenous carbonate rock systems. Are these methods applicable to large surface river basins with carbonate rocks but a heterogeneous lithology?

Literature Review

Caves, sinkholes, and disappearing streams are features often associated with karst environments; yet, few people are aware of the impacts of these landscapes in carbon sequestration or as a carbon sink. It is becoming increasingly important to understand and quantify carbon interactions within the environment, especially with increasing anthropogenic impacts on atmospheric CO₂ contributions from the burning of fossil fuels (Siegenthaler and Sarmiento 1993; Sundquist 1993; Falkowski et al. 2000; Cox et al. 2000; Doney et al. 2006; Liu et al. 2008, 2010). In response to increasing awareness about the environmental impacts of greenhouse gases, the public and political communities are increasingly reaching out to the scientific community for a greater understanding of the carbon cycle. This has resulted in expanding research toward better understanding processes associated with the carbon cycle. To understand the pertinence of extending research on the carbon cycle beyond its current bounds to include the relationships between two different carbonate environments, as well as aquatic vegetation on carbon budgeting, it is imperative to have knowledge of the relevant literature.

Carbon Cycle

Recent post-Industrial developments associated with significant increases in atmospheric CO₂ have resulted in numerous climatological and lithological studies; these have produced research involving both present day cyclic activities and those of the geologic past. James Hutton's classical theory of uniformitarianism suggests that physical processes occurring today were also occurring in the geologic past. An example of this would be fluctuations in CO₂, which are associated with environmental fluctuations that

occurred during changes between glacial and interglacial periods (Sigman and Boyle 2000; Lüthi et al. 2008). Naturally occurring Milankovitch cycles take place every 100 thousand years (ky), 41 ky, and 23 ky contributing to fluctuations between glacial and interglacial periods. These fluctuations are attributed to the orbital parameters eccentricity, obliquity, and precession, respectively (Sigman and Boyle 2000).

Using evidence from the Wisconsin glacial period (maximum extent 18 thousand years ago (kya)), Sigman and Boyle (2000) determined that during interglacial periods terrestrial environments act as carbon sinks, but this role is reversed during glacial periods. This phenomenon was likely due to the intrusion of ice sheets onto landmasses, which then prevented sequestration and resulted in an increase of atmospheric CO₂ (Sigman and Boyle 2000; Joos et al. 2004). Since then, approximately seven billion tons of carbon have been added to the atmosphere annually as a result of human activity (Liu and Zhao 2000). The so-called missing atmospheric carbon sink leaves some 3.6 billion tons of this carbon unaccounted for (Liu and Zhao 2000). During pre-Industrial interglacial periods, surface oceanic and atmospheric levels of CO₂ nearly balanced each other at 600 and 700 Pg C, respectively; post-Industrial Revolution anthropogenic impacts have altered this exchange. It is becoming evident that a drift is occurring from the natural cycle, leading to a break from the Holocene into what some are suggesting should be called the Anthropocene Epoch (Falkowski et al. 2000).

In assessing previous fluctuations in CO₂ and climate change, inferences can be drawn from ice cores regarding the impacts of anthropogenic activities. During the past 420,000 years, atmospheric CO₂ and temperature have reacted within a certain domain in which CO₂ fluctuated with 100,000-year cycles (~ 388 Gt C-- 596 Gt C). Recent post-

Industrial anthropogenic impacts have moved Earth out of this cycle and increased these levels to nearly 213 Gt C higher than previously witnessed through ice core records (Falkowski et al. 2000). High levels of CO₂ have reflected changes in temperature, as recorded through ice cores. However, the inverse of this has been shown not always to be true, as rapid changes in temperature are not always mimicked by changes in atmospheric CO₂ levels. Shackleton (2000) discussed phase variances with regards to CO₂ and ocean temperatures, noting 100,000-year variances as well as in-phase fluctuations with eccentricity. Post-Industrial impacts have altered this balance and atmospheric CO₂ levels as of the end of the 20th century were ~100 parts per million by volume (ppmv) higher, and concentrations had risen faster than previously found from ice core analysis (Falkowski et al. 2000).

Carbon dioxide is controlled, among other ways, through atmospheric exchanges with the surface water of the ocean. Chemical changes occur there and HCO₃⁻ is produced through reactions with CO₂. As dissolution of CO₂ occurs, it forms the weak acid H₂CO₃⁻ (carbonic acid) that then reacts with CaCO₃ when present, forming HCO₃⁻ along with calcium. The terrestrial weathering of rocks has provided cations to this system over a vast period of time; however, as CO₂ emissions from human activities increase, the ability of the surface oceans to absorb the CO₂ will likely decrease (Falkowski et al. 2000). Biological elements in the ocean also play a role in the cycling of carbon. In turn, they play a part in the “carbonate pump” by precipitating CaCO₃ into the deep ocean where a descending portion of certain phytoplankton and zooplankton shells are dissolved. This process then reduces oceanic surface dissolved inorganic carbon (DIC). The precipitation of CaCO₃ ultimately increases the dissolved CO₂ concentrations (pCO₂), while CO₂ is

circulated from the ocean to the atmosphere as a result of the carbonate pump on a century long time scales. Terrestrial landscapes can also serve as a sink; photosynthesis in plants, especially in forested areas, traps CO₂ and stores it (Falkowski et al. 2000; Cao et al. 2012). However, due to respiration/transpiration, this carbon is only stored for decades, although the carbon currently stored within vegetation is nearly three times higher (roughly 720 Gt for the atmosphere to the 2000 Gt in both living and dead biomass) than that of the atmosphere (Falkowski et al. 2000).

Large-scale carbon cycle models have typically assumed that the C sink from carbonate mineral dissolution on the continents is balanced with a source from mineral precipitation in the oceans. Carbonate rocks are the largest carbon reservoir on Earth, estimated at 6.1×10^7 Gt (Liu and Zao 2000). This necessitates a better understanding of how they function as reservoirs. The role carbonate rocks play in carbon fluxes also needs clarification through investigations into the biologic and atmospheric interactions that occur in the environments in which they are located (Liu and Zao 2000; Ludwig et al. 1999).

Many scientists are creating models to predict future CO₂ fluctuations; this has produced a variety of models of differing accuracy. The less accurate models tend to follow very closely to current knowledge of the carbon cycle, but often make broad generalizations that account for CO₂ relationships and do not delegate specific sources and sinks, such as aquatic vegetation. Models can only be as accurate as the information and understanding of relevant processes used to create them, so if information is missing in the carbon cycle, the ability of the model to predict future trends is affected. However, when modeling, it is common practice to test several models in an attempt to evaluate the impacts

of errors that may arise within the data. In evaluation of eleven models that represented the state-of-the-art in 2005, contradictions arose within the different model results in relation to the sensitivity of land and oceanic carbon uptake (Friedlingstein 2006). As a result, the researchers called for more observational data in order to “constrain” the models into a more “real-world” format. This type of on-the-ground approach will combine both locally specific data and modeling to better formulate a global carbon budget. The modeling approach toward CO₂ fluctuations allows researchers to initially take a more generalized approach toward the carbon cycle before focusing on individual aspects (contributors, sinks, or precipitators).

To categorize the carbon cycle into terrestrial, atmosphere, surface/ocean, and deep ocean is to generalize steps of the carbon cycle into their simplest forms. Each category is further broken down into sections that regulate how CO₂ is sequestered or released within these environments. An example of how this generalization can be reduced would be to consider the terrestrial environment, within which there are multiple types of lithological sinks that each play a different role in the carbon budget. A given mass of carbonate rock is capable of sequestering 17 times more CO₂ than silicate shield rocks and at least 10 times more than any other type of rock (Amiotte-Suchet et al. 2003). The budget for these environments also has to account for CO₂ uptake and release from terrestrial vegetation as it relates to photosynthesis, including respiration/transpiration.

Atmospheric CO₂ levels prior to the Industrial Revolution averaged around 600 Pg C (Sigman and Boyle 2000), though this changed dramatically after 1800. Since then, an average of about 7 billion tons of carbon have been contributed to the atmosphere annually as a result of human activity. Approximately 3.4 billion tons of carbon remains in the

atmosphere, while some 3.6 Gt is unaccounted for, and this missing sink has led to research to develop a more detailed carbon budget that will account for the discrepancy (Liu and Zhao 2000; Liu et al. 2008). Terrestrial sediments are the largest carbon sink, accumulating the majority of the CO₂ and in some cases storing it for millions of years. Following terrestrial sediments, abyssal waters are the next largest CO₂ reservoir with geochemical processes resulting in sequestration lasting an average of 1,200 years before releasing the CO₂ into the atmosphere (Liu and Zhao 2000). A great deal of research surrounding the epipelagic oceanic zone, in which photosynthesis can occur, and abyssal processes, as they relate to CO₂, has resulted in a relatively thorough understanding of these environments. However, a missing link arises in the relationship between the two environments and the proportional amounts of CO₂ entering the oceans through weathering processes. The proportion of CO₂ entering the ocean through rivers will fluctuate depending on numerous factors along the journey, some of which include lithology, vegetation (terrestrial and aquatic), soil, and temperature. Close examination of fluvial locations opens the door to expand upon the current literature available regarding the carbon cycle and CO₂ sequestration.

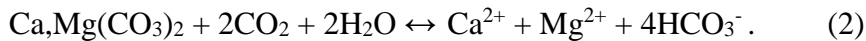
Some researchers are focusing first on individual aspects affecting a part of the cycle before taking into consideration the larger role they may play. This approach tends to provide a more complete look into a particular aspect of the terrestrial, atmospheric, or oceanic environments as well as encompassing how it fits into a global carbon scale. As mentioned, carbonate rock karst environments play a major role in carbon budgeting, therefore an in-depth knowledge of how these rocks impact the system is necessary (Yuan 1988; Liu and Zhao 2000; Groves et al. 2002; He et al. 2012).

Karst

Karst environments are those containing all physical parts of a geographic location, including the atmosphere, but are defined by the presence of the soluble bedrock (Yuan 1988). The lithology of possible karst environments can be categorized into siliceous (granite, quartzite, sandstone), evaporite (gypsum, anhydrite, halite), lava tubes (also called psuedokarst), but by far are dominated by carbonate rocks (limestone (CaCO_3) and dolostone ($\text{CaMg}(\text{CO}_3)_2$) (Palmer 2007). Dissolution is the primary method of chemical weathering for relevant reactions for carbonate rock in karst regions and can be described by the following reactions for limestone



and for dolostone,



Roughly 15 percent of Earth's ice-free land surface is covered by carbonate rock outcrops, including limestone and dolostone (Williams and Fong 2010). Karst aquifers have formed within many of these rocks that transport water through conduits formed by dissolution. These conduits are fed through fractures in the bedrock, sinkholes, sinking streams, and runoff that then percolates into the groundwater below or moves through the system until it reaches a local base level. Karst lithology is unique in that dual permeability and even triple porosity can exist (Worthington 2003) enabling dissolution and precipitation to occur throughout the system as the chemically active water reacts with the surrounding bedrock.

This information, in conjunction with the role that karst systems play in the carbon cycle, instigates a thorough investigation into these environments and the role they play in carbon sequestration.

Karst regions in Kentucky are well known, thoroughly researched, and home to the longest known cave system in the world (White and White 1989). Incision of the Green River has contributed to karst development in south-central Kentucky (Figure 1), in addition to relatively pure limestones and the gentle dip of bedding planes in this region (Dicken 1935; White and White 1989). Dicken (1935) subdivided the karst in this region based upon the landscape, with his “type IV” karst dominating the southwestern and southeastern portions of Green and Hart counties, respectively. Types Ic and II are dispersed in Hart County with Ic north of the river and II to the south (centrally located in the county). Type Ic, developed exclusively on limestone, is considered predominantly poorly developed karst with localized intensifications giving rise to more advanced karst. Dicken’s type II (doline karst) is the most typical found in Kentucky and is located within the St. Louis and in several places the Ste. Genevieve formation. The final subcategory of karst in this region is type IV and is typified by streams and basins developed on the impure Ft. Payne and Warsaw Formations (Dicken 1935). Both are relatively insoluble with impure limestones (shaly and siliceous) with outcrops of the Warsaw to the north of the river in Green County and the Ft. Payne to the south, and these are the dominant outcrops in the area (Grabowski 2001).

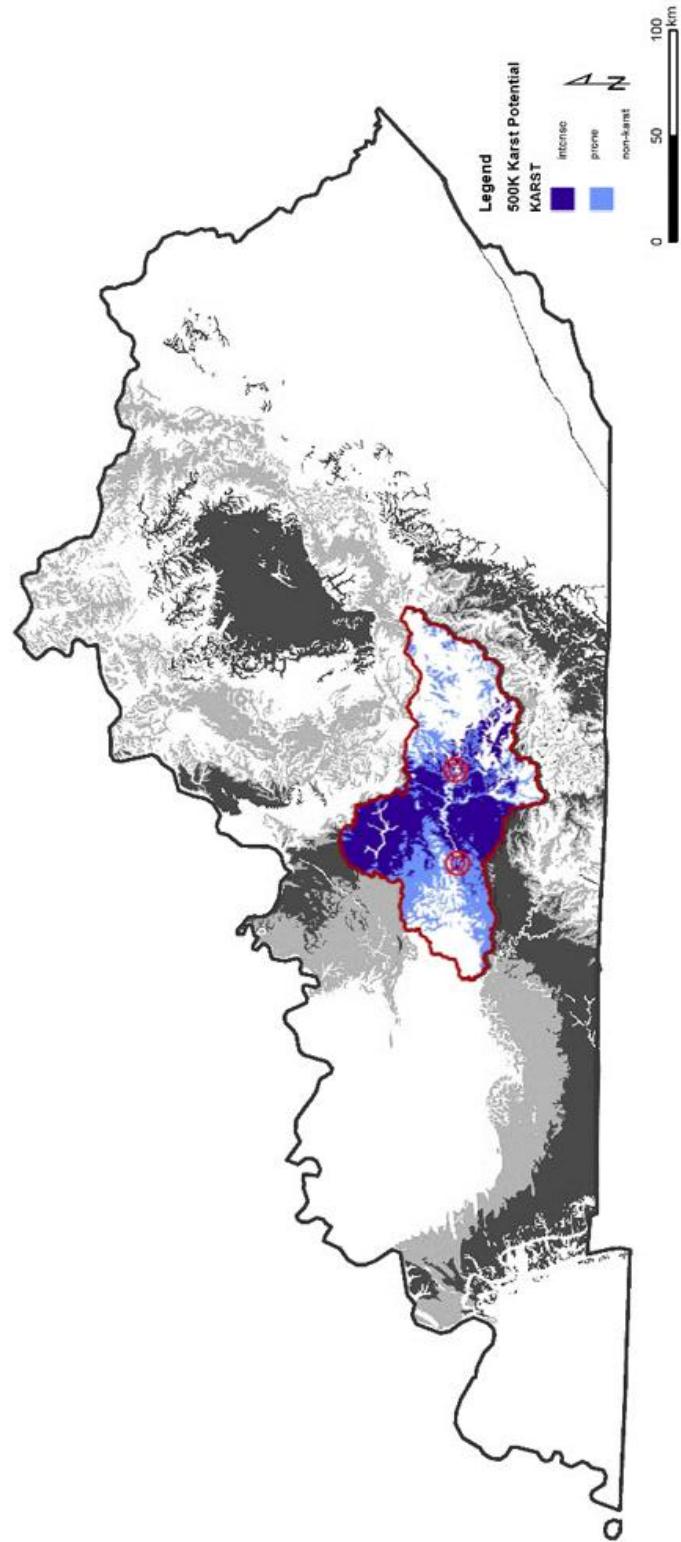


Figure 1- Karst in the Upper Green River basin. Source of karst data: Currens et al. (2002).

Since carbonate rock karst systems play a role in the global carbon cycle that has not been fully evaluated, it is necessary to have a thorough understanding of the lithology when monitoring for carbon fluctuations within an area. Ek (2004) studied hydro-geochemical and nutrient differences between adjacent watersheds that had varying proportions of karst and non-karst rocks. He investigated the Dry Branch and the First Creek watersheds within Mammoth Cave National Park, and determined that they were underlain by 47.7% and 12.2% carbonate rocks, respectively. This included measuring a number of variables, some of which included water sampling for a number of ions, temperature, pH, and discharge. The Ca^{2+} and Mg^{2+} ratios were both higher in the carbonate-rich Dry Branch watershed, which was associated with the larger amount of karst development in this area due to the higher percentage of carbonate rocks (Ek 2004). This is relevant to the study of the Green River because there are differences in the lithology underlying the Green as it flows from Greensburg to Munfordville. Karst landscapes become well developed as the river meanders westward, which is visible in Figures 2 and 3 as the occurrence of springs and sinks becomes increasingly dense westward through the watersheds. The underlying lithology becomes increasingly more homogenous, dominated by highly soluble limestone bedrock (Dicken 1935).

The carbon flux in a location can be complicated to measure due to the precipitation of calcite and competing dissolution processes (Liu and Zhao 2000). Limestone tablets have been used to determine dissolution rates within karst in conjunction with CO_2 fluctuations within a flow system. For example, Liu and Zhao (2000) collected data from several field sites from 1993-1995, which included limestone tablet weight loss, and hydrochemical data including pH, temperature, discharge, pCO_2 ,

Springs Located Within Watersheds

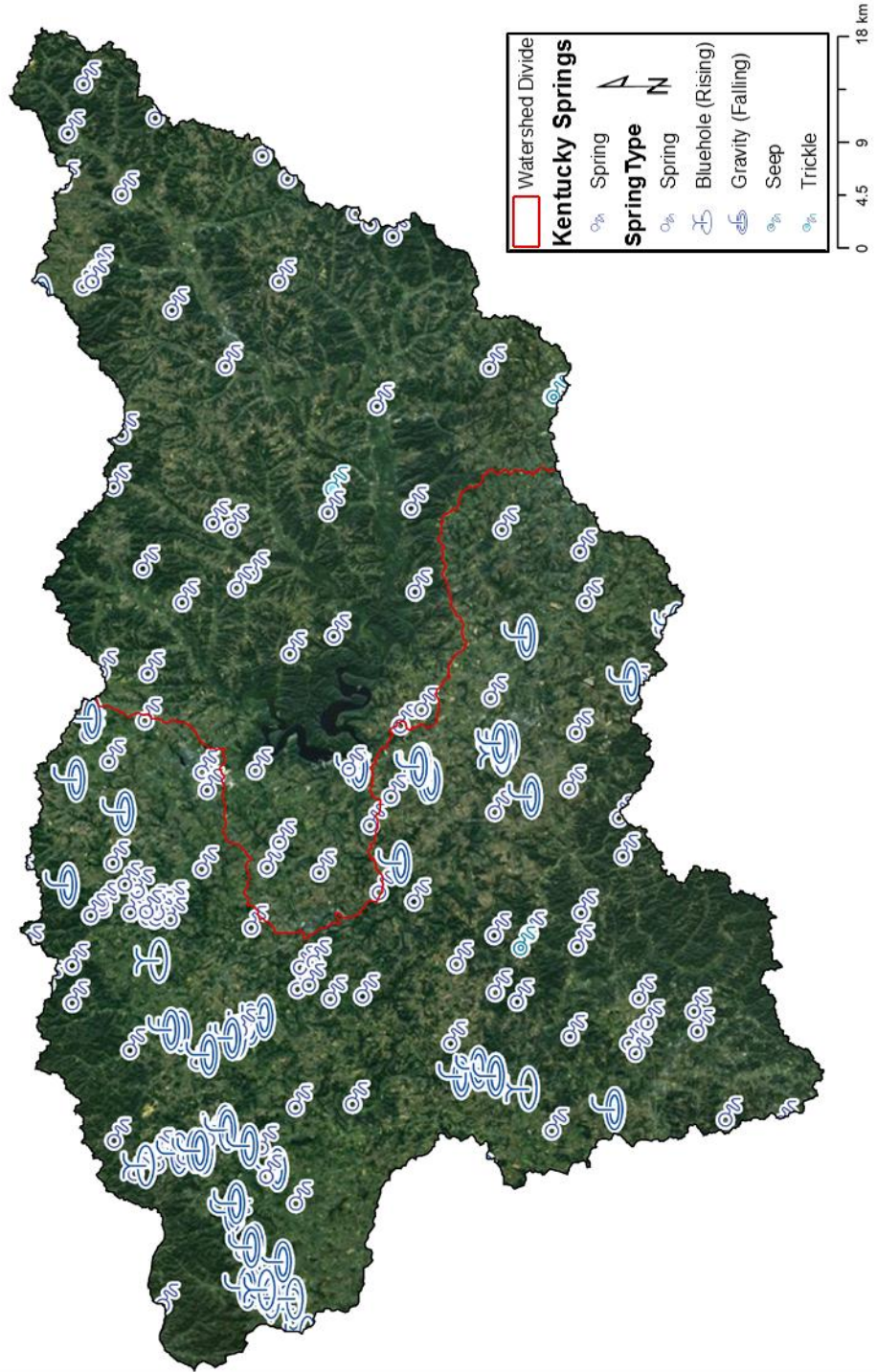


Figure 2- Springs Located Within Nested Watersheds of Upper Green River Basin. Source of spring data: KGS (2013).

Sinkholes Located Within Watersheds

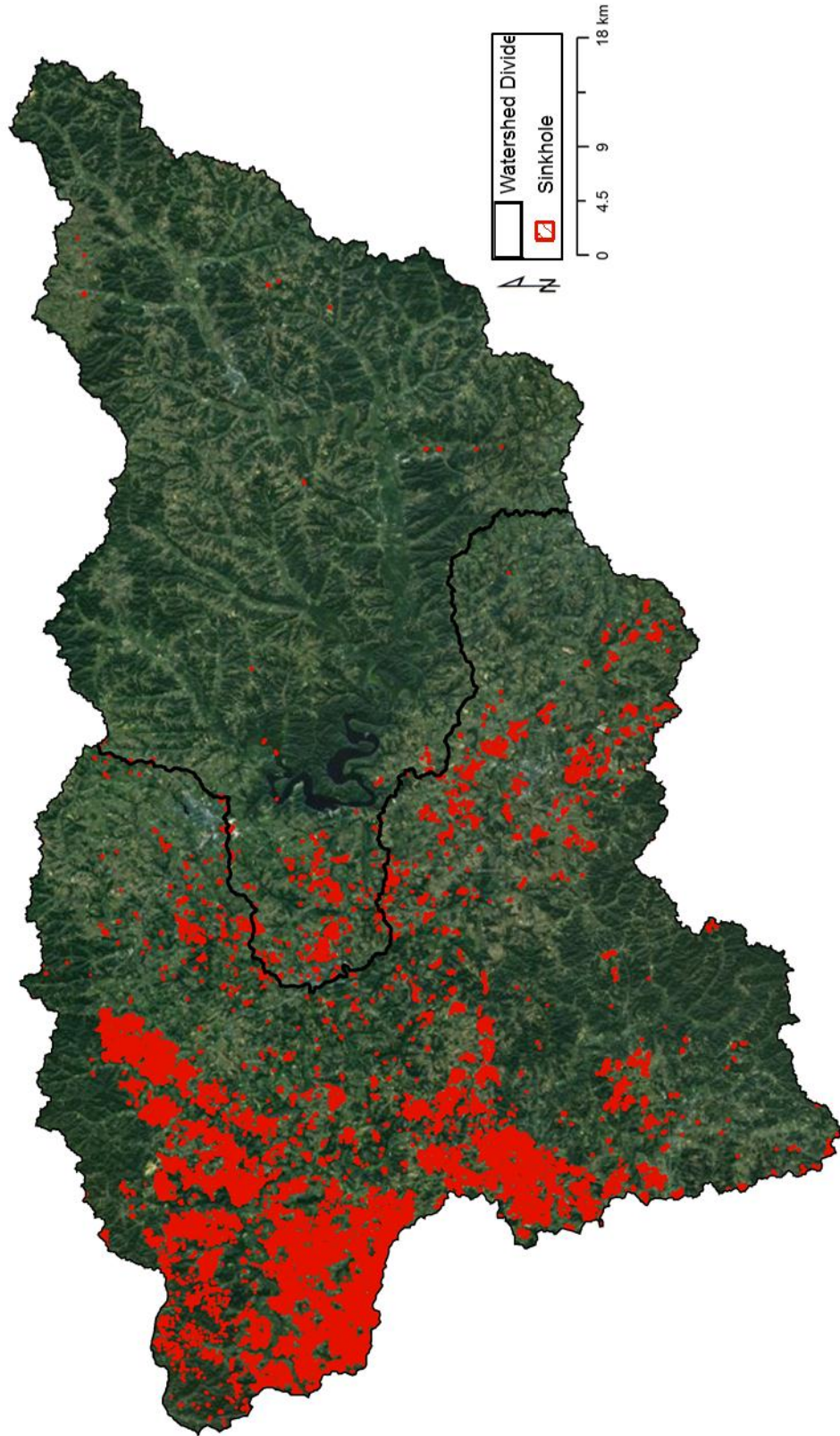


Figure 3- Sinkholes Located Within Watersheds of Upper Green River Basin. Source of sinkhole data:KGS (2013).

Ca^{2+} , and HCO_3^- . This information was then used to make a comparison between what they termed the “hydrochem-discharge” method and limestone tablet/soil data to decrease error prior to applying this information to the diffusion boundary layer model (DBL). Once quantified, an association to the global carbon flux was extrapolated from the data to arrive at an estimated net contribution of 0.11 billion metric tons through the hydrochemical-discharge method. The DBL model accounted for 0.41 billion metric tons of carbon with a precipitation (carbonate) value of 0.3 billion metric tons; however, these results differ from previous calculations, which they suggested would instigate additional studies (Liu and Zhao 2000). In analyzing the methodology used in this research, there are data unaccounted for within the carbon budget for the study areas. With regards to water chemistry and root uptake, TIC (total inorganic carbon) and DOC (dissolved organic carbon) were not quantified, nor was the impact of aquatic vegetation.

Heavy precipitation events were studied in the Lost River drainage basin in central Indiana, which provided an excellent collection site for samples and observations to formulate a four component mixing model for this karstic flow system (Lee and Krothe 2001). This model was then utilized to quantify influxes (rain, soil, phreatic diffuse flow, and epikarstic water) into the drainage basin. This research was relevant in reinforcing hydrologic concepts in karst environments, as well as the importance in data collection and storage. Their field research began in 1990 and continued through 1999, so gathering and storing data for long periods was instrumental in the success of this project. The four component mixing model approach may be an accurate way to quantify recharge into the drainage basin during heavy storm events; however, this is the only time period for which these data are accounted. The research did not attempt to expand this approach to include

intermittent periods with regular rain events, although an understanding of the overall recharge in a karst basin is required to determine geochemical fluxes for such basins, in particular regarding carbon fluxes.

Geochemistry

The geochemistry of water as it moves through karst landscapes is significantly impacted by water-rock interactions, including dissolution rates and potential sequestration of atmospheric carbon. In analyzing the geochemistry of a karst flow system, it should be noted that the values of temperature, pH, and SpC fluctuate with seasonal and climatological changes (Anthony et al. 1998; Groves and Meiman 2001, 2005; Liu et al. 2008). Research on the Logsdon River, Kentucky, provided high-resolution examples of such seasonal alterations, which were in some cases also affected by distance traveled by the water. In that particular case, outgassing (during summer sampling) caused by significant drops in CO₂ pressures due to interactions between the atmosphere and water in the cave occurred over the initial 4000m from upstream end of the underground river (Anthony et al. 1998). As a result, carbonate mineral precipitation was observed at this portion of the underground river. Also observed was an influx of CO₂ at approximately 5000m, although no definitive source was identified (Anthony et al. 2003). Values of SpC, as well as alkalinity, were both lower during winter months. While the research on the Logsdon was primarily in an underground setting, associations can be made to the seasonal changes that occur on the Green River. The methodology used by Anthony et al. (2003) can also benefit this study to distinguish specific geochemical changes during winter months, although this was not detailed in their work. Soil pH and climatologic data would be useful in assessing the seasonal changes in this area, as well as known recharge conduits

within the cave system that could alter the chemistry. In analyzing the geochemistry of a river system it is important to take into account as many variables as possible (dissolved inorganic carbon, dissolved organic carbon, particulate organic carbon (DIC, DOC, POC), and springs), as this is necessary when investigating changes that occur as water moves from one carbonate formation to another.

Significant concentrations of HCO_3^- can encourage photosynthesis in hydrophytes (plants adapted to grow in water); this can have an effect on carbon flux and can be investigated on a regional level. HCO_3^- is predominantly transferred through water, and large amounts are produced by the dissolution of carbonate rocks. Fluctuations in CaCO_3 between different carbonate environments may alter the rate of photosynthesis in conjunction with seasonal variations (Cao et al. 2012). These can be accounted for geochemically, by monitoring pH, SpC, Ca^{2+} , Mg^{2+} , HCO_3^- , and temperature. This, in addition to seasonal variability in karst environments, requires high-resolution data monitoring (He et al. 2012).

Discharge is one of the necessary measurements needed in monitoring geochemical fluxes, and several methods can be used to quantify this flux. Two standard methods for measuring discharge are to use a wading staff and flow meter, or the dilution method, which utilizes analysis of a breakthrough curve of an introduced conductive slug. Additionally, high precipitation events are monitored to determine the dominating hydrochemical variations during flood events as was demonstrated during research conducted by Liu et al. (2004).

Doctor and Alexander (2005) discussed the construction of a master recession curve to dissect the discharge data for interpretation. This provided the ability to address drainage

from the system, peak flows, and rates of discharge. The mean values of discharge (Q) and the drainage coefficient (α) were used to build the recession curve. The aforementioned methods are applicable in different aquifers, and could be beneficial in laying the groundwork for geochemical analysis and carbon budgeting on a regional scale. The application of these methods can enhance the current understanding of the geochemical conditions from different limestones within the study area on the Upper Green River, Kentucky including any mixing zones and the carbon partitioning within this system. However, for the research conducted, discharge was used predominantly for measuring the mass flux of carbon.

Raymond et al. (1997) conducted studies along the Hudson River in New York over several years and measured numerous parameters on a spatial and temporal scale to determine PCO_2 , conductivity, and pH. These data were in turn used to determine the carbon flux along the Hudson River. Studies were conducted on a diel, vertical, longitudinal, and seasonal basis to assess the hydrochemistry of the estuary. They identified a flux of $70\text{-}162\text{ g C m}^{-2}\text{ yr}^{-1}$ and a net respiration of phytoplankton of $293\text{ g C m}^{-2}\text{ yr}^{-1}$, which left approximately $100\text{-}192\text{ g C m}^{-2}$ unaccounted for.

Carbon Sequestration in Karst

Processes within karst environments may be particularly interrelated with climate change, due to the interconnectedness of CO_2 , H_2O , and HCO_3^- (Cao et al. 2012). This requires a thorough investigation into these environments to assess current and future carbon budgeting. Assessment of carbon fluxes in karst environments often requires a multi-method approach, as was the case with the study on the Logsdon River in south-central Kentucky, where in-situ field sites were arranged to collect data for the duration of

one year (Groves and Meiman 2001, 2005). Through this research, a great deal was discovered about karst water chemistry in the humid subtropical climate of south-central Kentucky. Data collected captured multiple heavy precipitation events that allowed for a differentiation of wet and dry seasons. These data included pH, Ca^{2+} , Mg^{2+} , TIC (total inorganic carbon), dissolution rates, as well as several other measurements to determine the inorganic carbon budget along with flow and saturation. The river remained oversaturated for 69% of the year, which under some conditions may have resulted in mineral precipitation within conduits during the dry season offsetting the wet season (Groves and Meiman 2001). After heavy spring storms, chemical base flow for the river was regained after months instead of days, as was river stage. The inorganic carbon budget for this area was found to be $7.8 \times 10^3 \pm 1.9 \times 10^3 \text{ kg ha}^{-1}$, the total inorganic carbon leaving the Cave City drainage basin. Of this, 57% was from carbonate mineral dissolution while the other 43% was from the atmosphere, either directly or temporarily stored as vegetation; however, organic carbon was not accounted for in this research.

In assessing the current literature available on the carbon cycle and carbon sequestration, gaps exist in the research, and there is a great deal of discussion involving terrestrial environments and lithology. Yet there is relatively little discussion regarding the differences in carbonate sinks and geochemical changes between the lithologies in these sinks. As previously mentioned, fluvial hydrophytes could also play an unaccounted for role in the sequestration process, by removing CO_2 from the system, which could result in an adjustment to carbon budgeting due to the abundance in aquatic vegetation in these environments. Hollander and McKenzie (1991) studied hydrophytes and carbon budgeting in a lacustrine environment. This research focused on fractionation in particulate organic

carbon (POC) $\delta^{13}\text{C}_{\text{poc}}$ and dissolved CO_2 with respect to increasing demands for carbon during high periods of photosynthesis that are generally seasonally driven (Hollander and McKenzie 1991).

Subaquatic biota were investigated on the karstic Ichetucknee River in Florida, in conjunction with diel fluctuations in hydrochemistry (Montety et al. 2010). The relatively short, yet high-resolution study, collected water samples for two one-week periods, and collection occurred at 4-hour intervals during the course of the study, except for one day in which samples were collected on the hour. During the same period, pH, dissolved oxygen (DO) and NO_3^- were measured in either 15 minute or 1-hour intervals. It was determined that the processes relating to the subaquatic vegetation directly correlated with carbonate mineral diagenesis, and they were the driving factor influencing in-stream diel fluctuations in this river (Montety et al. 2010). This was beneficial research in that it presented high-resolution data regarding the diurnal fluctuations of a section of river and the role aquatic vegetation can play in the hydrochemical processes that take place.

Carbon fluctuations in fluvial environments are pertinent in understanding the carbon cycle. As carbonate minerals are weathered and carbon is then released from terrestrial sediments it is carried through streams and rivers, and degassing of CO_2 into the atmosphere may also occur during this downstream transmission towards the ocean (Ciais et al. 2008). Various forms of inorganic and organic carbon are carried through the system in this process, and include DIC, $\text{CO}_{2(\text{aq})}$, PIC (particulate inorganic carbon) DOC, and POC. For carbonates, approximately 50% of DIC derives from the atmosphere with the other half coming from the dissolution of the rocks themselves. Ciais et al. (2008) noted

the provenance of the PIC in rivers is from mechanical weathering and has little effect on CO₂ budgeting, but should be noted.

Anthropogenic changes to fluvial environments should be accounted for in the total carbon cycle. Dams and reservoirs impact the flow of DOC and DIC to the ocean, and as saturation builds outgassing can occur and calcite may precipitate at some of these locations. In another example, research on algal mats on the Loire River, France has shown degassing from the mineralization of these mats after they were transferred into the estuarine turbidity maximum. This is a result of seasonal or annual consumption of atmospheric CO₂, and is attributed to land use ultimately increasing DOC in the fluvial system, therefore increasing the P_{CO2} and hydrophyte respiration. A positive relationship was noted between P_{CO2} and DOC in temperate Western European rivers (Ciais et al. 2008).

Chapter 2: Study Area

Background

The Green River is the largest tributary to the Ohio River in Kentucky with the valley covering approximately 24,423 km² within the state and 976 km² in northern Tennessee. The formation of the Green is attributed to the confluence of several small streams originating in the Appalachian foothills in Lincoln and Casey counties. From there, the river flows westward through both the Pennyroyal Plateau and the Western Kentucky Coal field. Along its journey toward the Ohio River, underground streams, as well as the Nolin River and Bear Creek, join the Green River. The lower reaches of the river become organized near Bowling Green, where the Barren and Green converge. The Green continues to the west from Bowling Green, prior to meeting the Ohio River between Henderson and Daviess Counties, and many other tributaries unite with the Green River (Crocker 1992).

Kentucky is well known for its karst landscapes, with approximately 25% of the state covered in well-developed karst. An additional 13% has some form of karst emerging, and 55% of the state is underlain by carbonate rocks with the potential for karst development (Figure 4) (Currens et al. 2002; KGS 2012). Of these karst landscapes, the most well developed are in south-central Kentucky; it is here that surface and subsurface drainage associated with the Green River act as a major agent in the dissolution of the carbonate rocks. The carbonate rocks in this region are Paleozoic in age and these shallow-shelf deposited marine sediments resulted from an epeiric sea when

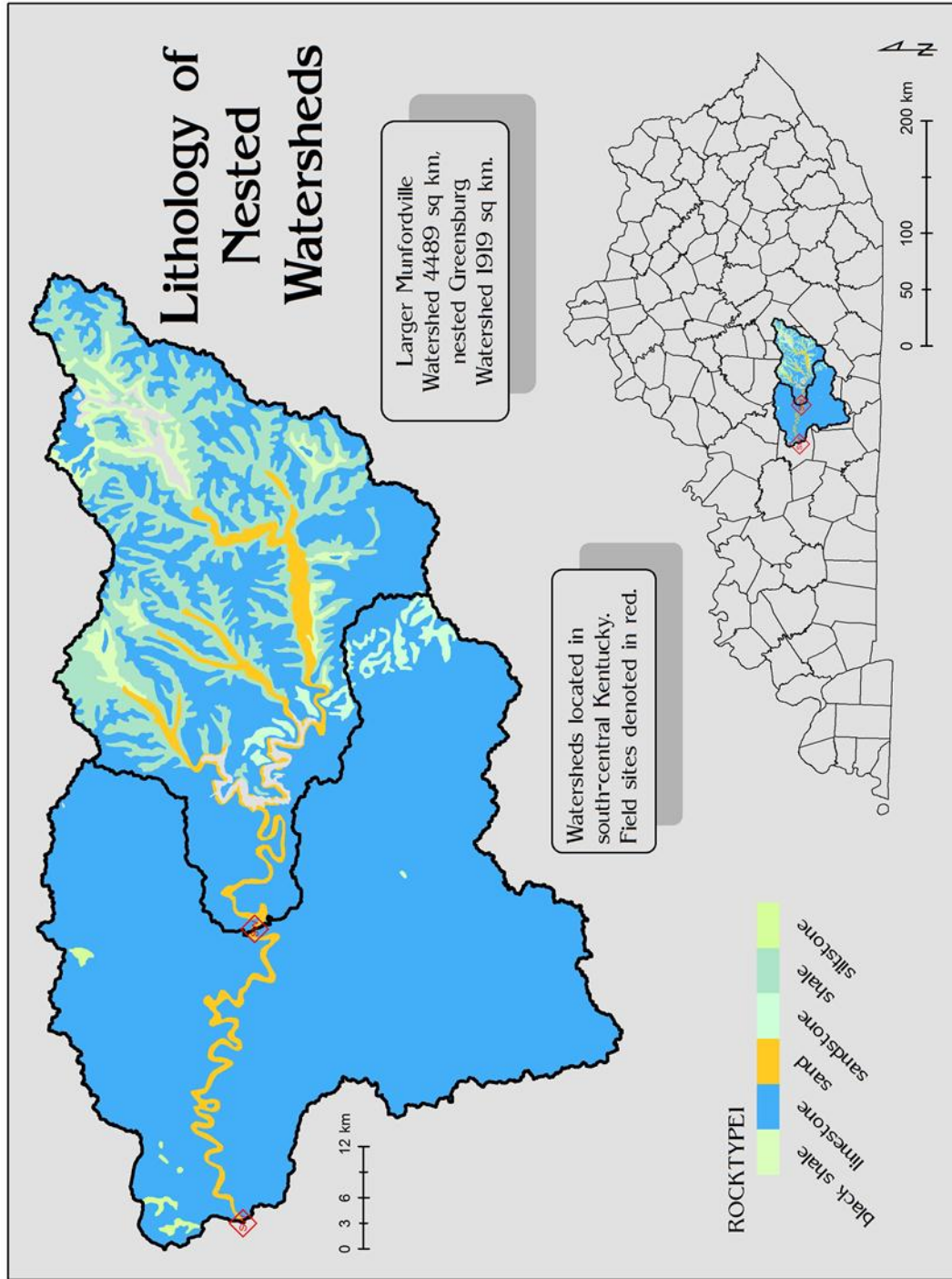


Figure 4- Map of Watershed Lithology. Source of lithology data: KGS (2013).

sea levels were high and intruded onto the land, and they have since been exposed due to weathering and sea level regression.

The lithologies of the two locations chosen for field sites are similar in many ways, but also differ in their constituents. The Greensburg site is located in the Ft. Payne Formation, Renfro Member (Grabowski 2001), Late Mississippian in age (approximately 330 my). Limestone in this formation ranges from thick-bedded and coarse-grained with crinoidal remnants to medium-bedded, fine-grained, slightly siliceous and unfossiliferous. Chert nodules are commonly seen within these beds, and can be present in the alluvium as a result of weathering, the beds are irregular and the bedding planes are uneven (Twenhofel 1931; McFarlan 1943; Grabowski 2001). The second field site in Munfordville, Kentucky, is located in the karstic St. Louis limestone, which is also late Mississippian in age. While the lower St. Louis Limestone is typically argillaceous, the upper half is relatively pure and forms well-developed karst. The formation is generally fine-grained and contains chert nodules. This limestone is primarily medium- to thickly- bedded and is underlain by the Renfro Member of the Ft. Payne (Twenhofel 1931, McFarlan 1943, Grabowski 2001) (Figure 5). Lithologic assessments of the watersheds for the two basins in the study area were addressed as the research progressed. This information was pertinent in determining the water-rock interactions to define the atmospheric sinks in these watersheds.

Estimates of basin lithology were based upon interpretations utilizing ArcGIS software and shapefiles obtained from the Kentucky Geological Survey (KGS), as well as groundwater flow and boundaries also obtained through the KGS (Currens and Ray 1998). In addition, hydrologic unit code files (HUC) from the United States Department

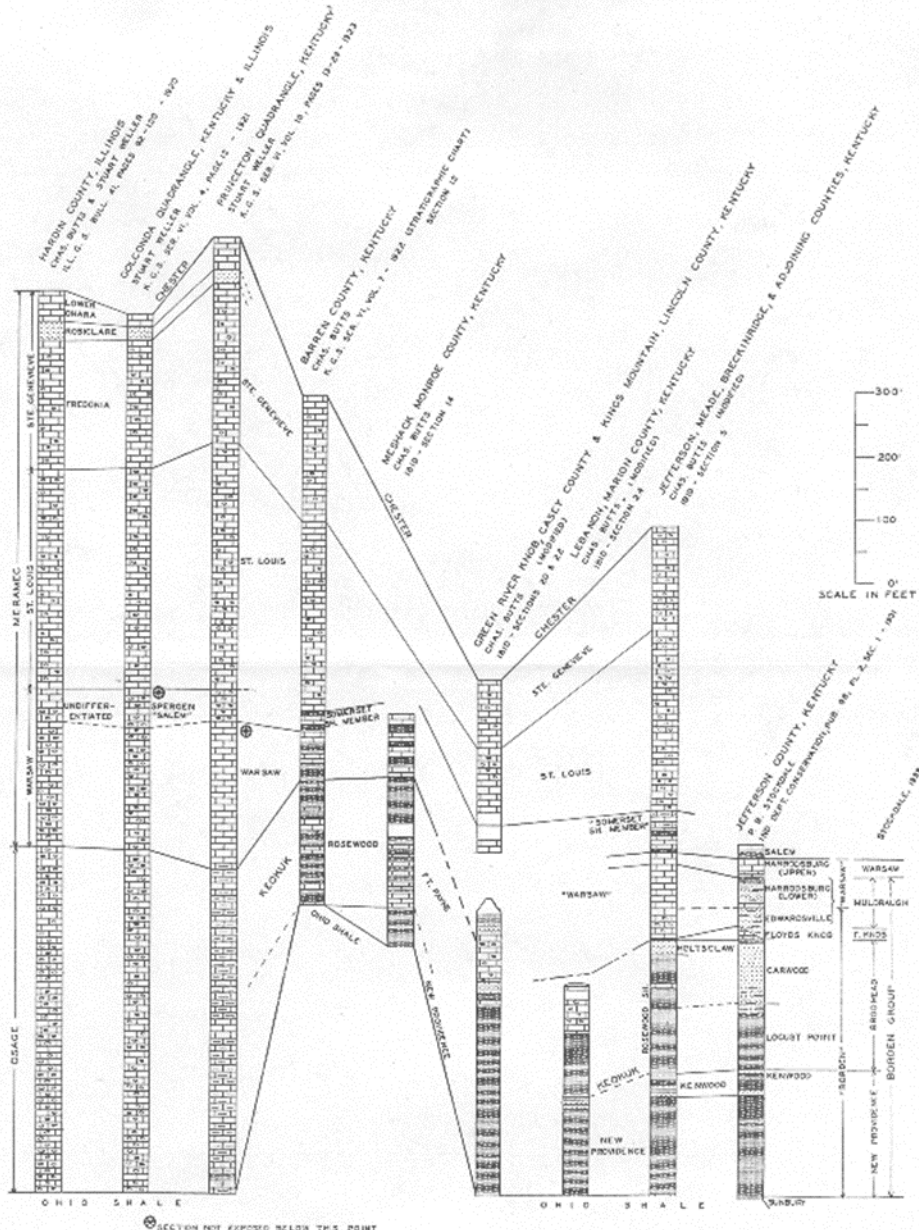


PLATE XVI
Lower and Middle Mississippian sections in western Kentucky

Figure 5- Stratigraphy of Region, Source: Kentucky Geological Survey (1939).

of Agriculture's Natural Resources Conservation Service (USDA 2013) were used. These files were assessed in ArcMap 10 to create basins upstream from the field sites. The lithology upstream from the Greensburg field site was found to have heterogeneous,

Mississippian limestones and Devonian and Mississippian shales dominating this basin with areas of 990 and 730 km², respectively. Smaller areas of the basin contain Pleistocene and Holocene sands (123 km²), followed by Ordovician dolostones and Mississippian sandstones of 26 and 23 km², respectively. The watershed upstream from the Munfordville field site encompassed the smaller Greensburg watershed, both totaling an area of 4,489 km² with the nested Greensburg watershed comprising 1,919 km² of the basin. This larger watershed is more homogenous with Mississippian limestones accounting for approximately 77% of the area within the basin (3,465 km²). Other lithologies in this watershed include shale (731 km²), sand (167 km²), sandstone (61 km²), dolostone (26 km²), and siltstone (13 km²).

Chapter 3: Methodology

High-resolution data were collected from October, 2013, to January, 2014, that provided insight into the hydrochemistry of this reach of the Upper Green River, including dissimilarities between the nested watersheds as well as daily fluxes for DIC and atmospheric carbon. Water samples were collected weekly from June 2013 through January 2014, while data loggers were installed and accumulated continuous data at 15-minute intervals from September (Greensburg) and October (Munfordville) 2013 through January 2014. High-resolution sonde data obtained from October 21, 2013, through January 27, 2014, were used for hydrochemical analysis of the watersheds; although additional data were obtained for Greensburg in September, 2013, these were considered to be supplemental. The additional data collected for Greensburg were a result of earlier placement of the multi-parameter sonde, therefore additional pH, water temperature, and SpC data were available for this location. All data were processed using Julian Dates with Alternate Julian Dates established to combine both 2013 and 2014 data sets. For this purpose the data set shown in the figures begins on October 21, 2013 and all dates thereafter are sequentially numbered.

Site Selection

This research was conducted at two field sites along the river. The first site was located in Greensburg (37°15'11.96"N, 85°29'59.51"W) and the second was in Munfordville, (37°15'57.68"N, 85°53'21.57"W) (Figures 6 and 7). Site selection was influenced by concern for the safety of equipment due to the extensive period of time it



Figure 6- Greensburg, USGS gaging station, (A) grab sample site (B) data logger site. Source: Photo by the author.



Figure 7- (A) Munfordville data logger site, (B) PVC encasements for data loggers. Source: Photo by the author.

was deployed, as well as ease of access and acquisition of data. To avoid loss or damage to the equipment, it was pertinent to choose sites along the river that provided security. The upstream site (Greensburg) was located near USGS gaging station 03306500. This gaging station also provided high-resolution data at 15 minute intervals, for precipitation, water temperature, and gage height. Grab samples were collected along the US 68 bridge, where the gaging station was positioned, although the site was established approximately 150 m upstream. The field site was located on private land, and as such permission was obtained for access for installation and weekly maintenance, where the data loggers were placed along the riverbank and situated so as to allow for unobstructed channel flow.

The downstream site, located in Munfordville, KY, was also situated on private property. This site was set up roughly 75 m downstream from the USGS gaging station, 03308500. Site security and accessibility were a consideration when choosing this location as it was within a few meters of a public park and boat ramp. However, the data logger was installed on private land where fencing and signs assisted in limiting pedestrian traffic near the equipment. As was the case in Greensburg, the sonde was positioned in the river to allow channel flow over the probes. For both sites, it was necessary to take into account the placement of the sondes in the river, as channel flow was optimum it was also pertinent to keep the sondes near the bank to prevent damage from both river traffic and debris. In doing this, the loggers were set up approximately 1 – 1.5 m from the bank to eliminate the possibility of backflow.

Water (grab) samples were collected weekly for both Greensburg and Munfordville. The grab samples were obtained in Greensburg from the west side of the bridge on US 68 (South Main Street) (Figure 6-A). This location was chosen because it

allowed for the samples to be taken from of near the center of the river. This was also a prime location due to the close proximity of the gaging station (within a few meters, Figure 8). Although the ideal location for water samples to be collected was from the center of the river, this was not always possible in Munfordville. The bridge nearest to the field site was inaccessible due to high traffic volumes and poor pedestrian access. At this site it was necessary to wade to the center of the river to obtain the samples when the river was near base flow. During high flow, taking samples from the center was not an option; thus, samples were taken along the bank (the boat ramp, Figure 9). The 50 km distance between sites allowed for determinations of hydrochemical variation along the reach due to hypothesized biological and lithological variations.



Figure 8- Greensburg field site. Source: www.google.com/earth.



Figure 9- Munfordville field site. Source: www.google.com/earth

Site Installation

Site security and accessibility were major considerations in the design and construction of the field sites. The data loggers needed to be protected from outside influences including riverine debris, high flow conditions, and human interference. The conditions at both sites changed rapidly during large dam releases, as well as local events, introducing both precipitation and increased outflow from groundwater inputs. During these events, water levels continued to rise over periods of hours and days until equilibrium was reached and the water levels fell again. In order to maintain access and protect the equipment, 10 cm PVC pipes were installed to house the loggers (Figures 6-B and 7-A). The length of the pipes differed depending upon the bank slope of the location; Greensburg, for example; required approximately 11 m of PVC; while in Munfordville it was necessary

to install close to 18 m. The length of the pipes allowed access during most high flow events, while also ensuring the probes reached adequate channel flow. There were occasions in which high flow denied accessibility to maintaining the loggers, due to fluvial incursion onto the flood plain covering pipe opening making acquisition of data hazardous. The pipes were secured using concrete filled cement blocks, hose clamps, and 1.5 m tee fence posts. Pipe couplers were utilized to connect the pipe sections in addition to PVC caps (10 cm) to enhance security. The caps prevented access to the sondes by outside parties; holes were drilled into the caps to install a thin metal bar that housed a lock. Aircraft cable was attached to the caps and the internal PVC encasements and was set to run the length of the pipes, this allowed for placement and removal of the encasements/sondes from the pipes. The encasements were constructed using 5 cm PVC pipes with couplers and caps; they were divided into two sections with the bottom filled with lead shot and the top held the loggers (Figure 7-B). The shot was used to provide additional weight; this was beneficial in lowering the encasements through the pipe and into the water. Holes were drilled in the encasements, which introduced water from the river to the probes on the sondes, serving as a stilling well. Holes were also drilled on the outside PVC pipe to equilibrate the inside pressure with that of the outside air as well as to introduce water flow into those sections in contact with the river. A drain was placed along the bottom of the pipe and provided for water flow through it to the encasements. The PVC pipes were attached to 2x4's that were drilled to trees at both locations; this provided additional stability for the pipes. The cement blocks were placed both in the center of the pipes, where pipes were vulnerable to bowing and at the base of the pipes. The tee fence posts were placed in concrete in the cement blocks and hose clamps were used to strap these to the

pipes. These installations were designed to provide maximum security with minimal disruption to the property.

Mapping Methods

Maps were created prior to, and during, data analysis to determine the lithology of the watersheds as well as their boundaries. It was essential to obtain this information since lithologic elements impact the hydrochemistry of the river, and basin boundaries were needed to determine inputs into the system and were vital in quantifying the carbon sink for each watershed. It was necessary to procure maps and shapefiles from outside sources in order to calculate the geometry of each watershed and create maps relevant to this study; these were obtained from several sources including the KGS (2013) and USDA (2013).

Prior to analyzing any data, basin boundaries needed to be delineated. This was accomplished through editing new layer files in ArcMap 10. The basin was delineated by using the editing tools and drawing the basin outlines while interpreting the topography on 7.5-minute quadrangles (KGS 2013), as well as pre-delineated basins, including HUC files (8, 10, 12, USDA, 2013), groundwater basins boundaries, and groundwater flow files (KGS and Kentucky Division of Water). During this processes, it became clear that some of the HUC basins did not account for the groundwater flow or basin boundaries. This was most prominent along the western borders of the Munfordville watershed, where the HUC boundaries crossed over the groundwater basins multiple times (Figures 10 and 11). Although ArcGIS has several tools that are useful in delineating basins, it was necessary to draw these by hand in ArcMap to address issues that occur in karst

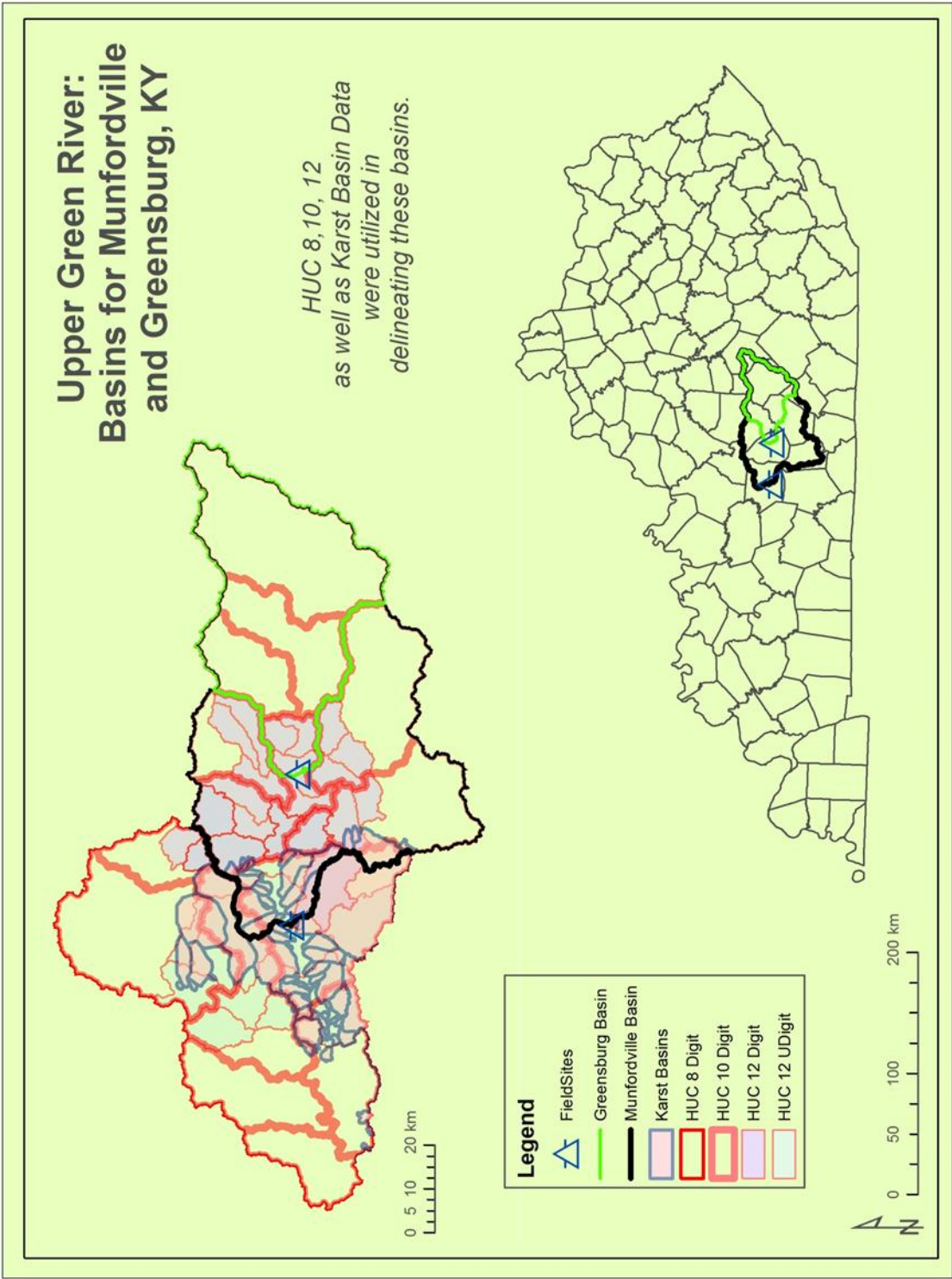


Figure 10- Upper Green River Study Area Basin Boundaries. Source: Created by author.

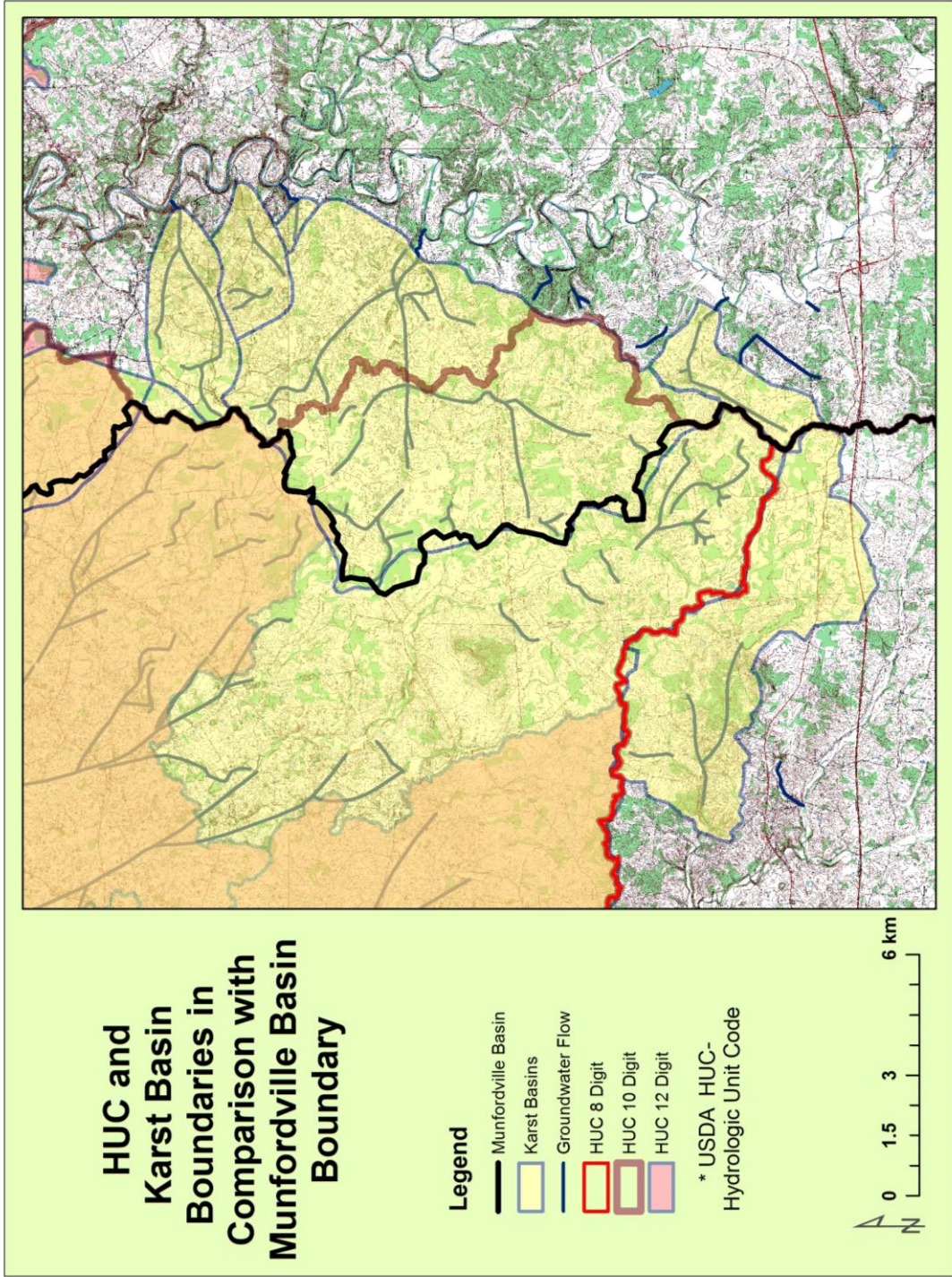


Figure 11- Basin Boundary Comparison, Munfordville. Source: Created by author.

regions, including sinkhole inputs and groundwater flow. Interpreting boundaries in these environments necessitated the use of all the above mentioned files (karst atlas and HUC files) in addition to considering the topography of the region.

Once the basin boundaries were delineated (Munfordville and Greensburg), it became possible to determine their areas and lithologies. To calculate these variables, the linear basin shapefiles were changed into polygons with the Feature to Polygon tool in ArcMap. The basin polygons were then spatially joined to the Kentucky Geology polygon, obtained from KGS, and this process ensured that metadata from the geology feature to become an attribute of the new joined shapefile. The new shapefile was then clipped with the Geoprocessing Clip Tool in ArcMap to the basin polygons. Symbology on the clipped file was set to portray the primary lithology (Rock Type 1) from the geology shapefile. New fields were then added to the attribute table of this new file to differentiate between rock types and for the calculation of the area of these types within the basins. This was accomplished through selecting each set of attributes applicable to each rock type; they were then assigned a number to differentiate each lithologic set. Geometry was then determined based upon the new boundaries and input into a new column within the attribute tables. The area of each rock type was calculated based upon metadata from the original KGS lithology shapefile and was summed for each lithology typed present within the watersheds. These data were then verified with those of the total geometry of the watersheds to ensure accuracy. Datum for shapefiles and base layers varied; however, these were projected in NAD 1983 State Plane Kentucky South FIPS 1602 Feet.

Sample Collection

Water samples were collected on weekly intervals and during high and low discharge events. The samples collected during high/low discharge events were collected randomly during normal weekly sampling events as well as specifically using ISCO automatic water samplers to obtain a range of SpC values with correlating HCO_3^- measurements. Grab samples were analyzed for Al^{3+} , Ca^{2+} , Cu^+ , Fe^{2+} , K^+ , Mg^{2+} , Na^+ , P^+ , Pb^{2+} , S^+ , Zn^{2+} , HCO_3^- , F^- , Cl^- , NO_2^- , Br^- , NO_3^- , PO_4^{3-} , and SO_4^{2-} . Water sampled for cations, anions, and bicarbonate was filtered using a syringe, filter holder, and $0.45\mu\text{m}$ paper filter. The samples were filtered into 60 mL (cations and anions) and 250 mL (alkalinity) bottles with no headspace and wrapped with Parafilm. The cations were preserved at a pH of 2 or less with nitric acid (HNO_3) prior to refrigeration at 4°C until processing occurred (Jackson 2000; EPA 2012). In the field, all water samples were placed in an ice-filled cooler once collected. The hold time for most cations and anions is 28 days; however, for nitrite, nitrate, and phosphate it is only 48 hours. Therefore, anion analysis was completed within this 48-hour window and cations were analyzed within 28 days of collection (Jackson 2000; EPA 2007). Bicarbonate was analyzed initially (July through November 2013 data collection) in the Hoffman Environmental Institute's Field Laboratory, as well as in the Waters Laboratory, Bowling Green, KY (November 2013 through March 2014), using standard method 2320b within 24 hours of sample collection (Waters 2009; EPA 2012).

Grab samples at the Greensburg field site were collected in clear PVC bailers lowered using a reel and string from the center of the US 68 bridge in Greensburg. The water was then transferred into two 500 mL Nalgene bottles for ease of filtration into 250 mL sample bottles, in addition to obtaining grab sample data with a handheld YSI 556 multiparameter

probe (pH, SpC, and water temperature). Grab samples obtained from the Munfordville field site were taken along the bank during high flow conditions and from the center of the river during base flow. As previously discussed, these samples could not be procured from the bridge at this site due to safety risks. These samples were collected in two 500 mL Nalgene bottles prior to filtration and grab sample data collection by the YSI 556 multimeter. Samples from both field sites were filtered and transferred into appropriate bottles (acidification using HNO_3 for cation samples) in-situ.

Water sampling also occurred during events in which water levels changed either to high flow conditions or those returning to base flow so as to obtain HCO_3^- samples with a range of SpC values. During the course of this data collection, one ISCO 6712 automatic water sampler was stationed at each field site. These were set to take 850 mL water samples on four hour intervals. Samples from these automatic samplers were collected on a two-hour resolution and processed in the laboratory within the appropriate hold times for bicarbonate (Jackson 2000; EPA 2007). The ISCO samplers were set to collect 500 mL of the available 1000 mL in the sample bottles to prevent cross contamination in the event excess sample was collected from the ISCO. Due to the extended distance from Western Kentucky University, as the field sites are 50 km apart, it was not possible to collect the samples with no headspace until they were filtered and transferred into separate 250 mL sample bottles for each time period collected by the ISCO. The samples were transferred to bottles, where this issue was alleviated within 24 hours of their collection. Additional high/low discharge event sampling occurred over a 2.5 week period (time constraints prevented prolonging the sampling beyond this period). During this round of sampling, the ISCO automatic water samplers were set to collect 500 mL samples at two-hour intervals.

The samples were then collected within 24 hours (generally within 8-12 hours), and then measured for differences in SpC. Those samples with varying SpC ranges were then titrated for HCO_3^- concentrations. Although it was preferential to filter, record SpC readings, and limit headspace at the time the samples were taken, due to field-site location and length of time between samples, sample collection with these parameters was not feasible. Ultimately only two samples proved to be beneficial and were utilized in the data set, as all other samples collected had similar SpC values to those at the time of high/low discharge collection preventing the need to titrate for HCO_3^- as these measurements would have been comparable to the samples previously recorded in the data set. Limitations in this sampling also included changes in discharge which resulted in restricted chances for data collection over the 2.5 weeks the automatic samplers were placed at the field sites. This sampling was only considered supplementary to weekly sampling events and was utilized to strengthen ionic relations between HCO_3^- and SpC.

High-resolution data collection occurred at each field site through the installation and maintenance of YSI 600 XLMs multiparameter data sondes. Three YSI 600 XLMs were used for this research; two were placed at the Greensburg field site and one at the Munfordville site. The data loggers at both field sites were set to collect pH (both in instrument calibration pH units and in mV), SpC, water temperature, and one logger also recorded depth (blue logger, placed at Greensburg). These were set to record measurements at 15-minute intervals so as to correspond with USGS gauging station data collection. This collection interval was intended to prevent data entry errors and to simplify interpretation during data analysis. The data from the data loggers were downloaded and maintained on a weekly basis, which provided for weekly interpretations and limited drift on the probes

through frequent calibrations. Data were downloaded onto a laptop prior to calibration or cleaning of the probes, and were later transferred into both Excel and SigmaPlot for analysis.

Calibration of the pH probes occurred weekly to minimize drift and to formulate linear regressions for pH analysis. Calibration of these probes was completed by initially rinsing the probes with deionized water to remove silt and biological elements. The clean probes were then rinsed in pH 7 buffer then placed in a cup of 7 buffer until equilibrium was reached and the calibration was recorded, this process was then repeated for the 4 buffer followed by the 10 buffer. The procedure for calibrating the pH probes was based upon the 6-Series Multiparameter Water Quality Sondes User Manual. This determined the order in which the probes were introduced to the buffers as well as the time frame for calibration (weekly calibrations with time per buffer depending upon the rate of equilibration within the buffers). The pre-rinse in pH buffer was a recommendation made by YSI personnel over phone as a preliminary step to reach equilibrium for calibration and reduce variations in calibration values.

The in-range calibration values fluctuated from 0 ± 50 , 180 ± 50 , and -180 ± 50 , respectively for buffers 7, 4 and 10. Calibration values were recorded on a field sheet then inserted into SigmaPlot data processing software during data processing to develop regressions. Calibration of SpC was also required to prevent the drift of these probes as well; however, the calibration for SpC was not required on a weekly basis. Fondriest Environmental (2006), the manufacturer, recommends calibrating SpC probes seasonally but cleaning them often. Therefore, the SpC probe on each sonde was cleaned with a wire YSI brush bi-weekly at a minimum. Calibration was initially conducted prior to

deployment of the sondes and repeated once every three months. Calibration was accomplished using techniques outlined in the 2006 6-series Multiparameter Water Quality Sondes User Manual. This process involved placing these probes in conductivity solution for a minimum of 60 seconds prior to initializing the calibration process. This procedure allowed the sondes to equilibrate to the temperature of the solution. Temperature plays a role in SpC and can cause up to a 3% change in SpC per change of one degree Celsius (Fondriest Environmental 2006). When the probe became accustomed to the temperature, calibration commenced in 447 μ S conductivity solution. Upon completion, all probes were thoroughly rinsed in deionized water and deployed.

In addition to calibration, cleaning of the pH probes was necessary to prevent buildup on the bulbs from siltation and biologic influences (i.e. algae). Electrode cleaning solution was utilized in this process as well as deionized water. Prior to cleaning, data were downloaded and the probes were calibrated. The pH probe was removed for cleaning to prevent the occurrence of fouling on the other probes (SpC and temperature). The probes were soaked in the electrode cleaning solution for no less than 30 minutes and no more than one hour. Although probe cleaning normally necessitates eight or more hours for this process, due to field site location and the ability to maintain high-resolution data acquisition, it was necessary to limit the time in which the probes were cleaned. Once cleaned the probes were thoroughly rinsed with deionized water and re-calibrated prior to the reattachment of the probe to the logger. Once all downloading, calibrating, and cleaning of data loggers was completed they were set to record data at 15-minute intervals and redeployed. The pH drift often occurred after probe cleaning so it was necessary to limit

the cleaning sessions to every six weeks. This provided ample time for re-equilibration of the probes yet prevented them from acquiring a great deal of build-up.

Laboratory Analysis

Three laboratories were utilized to process the grab samples. Anions and cations were analyzed at the Advanced Materials Institute (AMI), while bicarbonate was titrated initially at the Hoffman Environmental Institute's Field Laboratory, then at the Waters Laboratory. Analysis of anions was conducted at AMI using Chromeleon software and Ion Chromatography (IC) on a Dionex IC (EPA method 9056). Ion Chromatography was used to determine concentrations of fluoride, chloride, nitrite, bromide, nitrate, phosphate and sulfate (F^- , Cl^- , NO_2^- , Br^- , NO_3^- , PO_4^{3-} , and SO_4^{2-}) in the aqueous sample. Standards were run weekly prior to sample analysis, the standards included three blanks (eluent: sodium carbonate), one prior to analysis, one following the standards and a final at the end of the run to ensure no carryover from the site samples remained in the column. An anion standard solution containing the seven anions previously discussed was diluted to form six individual standards (.3, 1.5, 3, 6 and 9 ppm) of chloride. The samples were run weekly and within 48 hours of collection to meet EPA standard hold times for nitrite, nitrate, and phosphate (EPA 2007) (Figure 12). Once analyzed, calibration standards were examined for retention time and peak height prior to verifying these parameters for the grab samples. The data were then exported to an excel spreadsheet the data were then imported into Sigma Plot for analysis.

Analysis of cations, including, aluminum, calcium, copper, iron, potassium, magnesium, sodium, phosphorous, lead, sulfur and zinc (Al^{3+} , Ca^{2+} , Cu^+ , Fe^{2+} , K^+ , Mg^{2+} , Na^+ , P^+ , Pb^{2+} , S^+ , and Zn^+) was conducted on an Inductively Coupled Plasma Emission

Analyte	Preservation	Holding time (days)
Acetate	Cool to 4 °C	2
Bromate ^a	Add 50 mg L ⁻¹ EDA ^b	28
Bromide	None required	28
Chlorate ^a	Add 50 mg L ⁻¹ EDA	28
Chloride	None required	28
Chlorite ^a	Add 50 mg L ⁻¹ EDA, cool to 4 °C	14
Chromate	Adjust pH to 9–9.5 with eluent ^c	1
Cyanide	Adjust pH to >12 with NaOH, cool to 4 °C	14
Fluoride	None required	28
Formate	Cool to 4 °C	2
Nitrate ^d	Cool to 4 °C	2
Nitrite ^d	Cool to 4 °C	2
<i>o</i> -Phosphate	Cool to 4 °C	2
Sulfate	None required	28
Ammonium	Filtration, cool to 4 °C	7
Calcium	Filtration	42
Magnesium	Filtration	42
Potassium	Filtration	42
Sodium	Filtration	42
Metals, e.g. Co, Ni, Zn	Acidify to pH < 2 with nitric acid, i.e. 1.5 mL conc. HNO ₃ per liter sample	6 months

Figure 12- Hold time for anions (Jackson 2000).

Spectrometer (ICP). This tested for the concentration of selected cations in the water samples, providing these concentrations in parts per million. Standard methods (EPA method 200.8) were followed to process samples on this equipment as well (Long et al. 1994). Standards and blanks (3-5% nitric acid solution) were also utilized in each run of samples. Samples were run both in normal concentrations and 1:10 diluted concentrations. This was necessary due to the high Ca²⁺ levels in the samples from both sites that generally exceeded the highest standard concentrations. The samples were diluted using a 3-5% nitric acid solution with 1 ml of sample to 9 ml of solution. Samples were analyzed within the 28-day hold period, which required a monthly sample run on the ICP-ES for several sample dates. Once analyzed, calibration standards were observed and verified prior to any post

processing to insure accuracy of the wavelengths and concentrations observed for the samples.

Water is electrically neutral; therefore, if all cations and anions present in the sample were analyzed perfectly and their charges summed the result would be zero. However, since the sampling for this research did not require analysis of all potential ions in the river at the sampling sites, a charge balance check was beneficial in determining accuracy of the laboratory analyses. Cation and anion data were compiled for each sample date in an Excel spreadsheet where they were converted from ppm to milliequivalents per liter (meq/l). The cations and anions were then summed and input into the following equation:

$$CB \% = (cations - anions / cations + anions) * 100. \quad (3)$$

Where $CB\%$ is the charge balance error expressed as a percentage. Murray and Wade (1996) suggest a typical acceptable error range of $\pm 5\%$, though we accepted a range of $> \pm 7\%$ for this research, with 114 total samples where 23 samples $> \pm 5.5$ > 91 samples. Because bicarbonate so dominates the anions in the waters of both sites and has concentrations much higher than any other anion, relatively small variations in the accuracy of the bicarbonate titrations can have a relatively large impact on charge balance errors. Because the charge balance errors were not dominated by either anion or cation deficits, this is likely the principal reason for what charge balance errors that exist, rather than a particular cation or anion that was not included in the analysis.

In carbonate rock-dominated systems, bicarbonate can be assumed to be equal to the alkalinity of the water (Amiotte-Suchet et al. 2003). Using this assumption, bicarbonate was titrated (Method 2320B) in both the Hoffman Field Laboratory and the Waters

Laboratory. The 250 mL bottles used for alkalinity supplied enough of the aqueous sample to titrate these grab samples a minimum of three times per site at 50 mL each. Titrations were completed using a 50 mL burette, a 100 mL beaker, a 100 mL graduated cylinder, sulfuric acid (H_2SO_4) and a Hach HQ40d meter with attached pH C101 electrode. The additional 100 mL in the sample bottles was used in the event an error occurred during titrations. The sample was poured into a graduated cylinder prior to pouring it into the beaker to ensure each sample analyzed was 50 mL. The probe was then permitted to stabilize before initial pH, temperature ($^{\circ}\text{C}$) and milliliter readings (titrant, H_2SO_4) were recorded. The sample was then placed under the burette and the titration commenced. H_2SO_4 was added to the sample until the pH was approximately 4.50, with an acceptable error range of 10%, once this pH was reached final pH, temperature and titrant milliliters were recorded. This was then repeated so that each sample site had three HCO_3^- values for each field site. For situations in which the final pH reading for any sample was less than 4.40, the titration was repeated and the new readings replaced that of the previous titration. All readings were initially recorded on a paper spreadsheet prior to transferring these into an Excel spreadsheet designed to calculate HCO_3^- in mg/L. The calculations applied in the Excel spreadsheet were obtained from the Waters Laboratory, to maintain consistency with their procedures.

Data Analysis

Analysis in the office included the importation of data from data loggers (YSI 600XLM) into the Sigma Plot software package, and graphing fluctuations in pH, SpC, temperature, discharge, cations and anions against time. Time series and multivariate

graphing provided for examination of multiple variables on one graph so comparisons could be drawn with ease. Linear regressions were used to determine the statistical relationship between SpC and Ca^{2+} , SpC and Mg^{2+} , and SpC and HCO_3^- , and were processed in SigmaPlot.

Data processing included the averaging of pH data from the two data loggers placed at the Greensburg field site (labeled Orange and Blue). The pH data were graphed for both loggers and examined to determine any discrepancies between them. Differences between the loggers ranged from approximately ± 0.1 - 0.7 , with the majority falling into the lower range. The data from these loggers were then averaged and graphed for comparison with the two loggers and the data used for further examination into the hydrochemistry of these nested watersheds (Figure 13). Differences between the probes placed at Greensburg were found to be minimal and ranged from approximately ± 0.1 - 0.7 , with the majority falling into the lower range. The data for these loggers were then averaged and graphed for comparison with the two loggers and the data used for further examination into the hydrochemistry of these nested watersheds.

Continuous SpC data were also collected from the two sondes placed at the Greensburg field site; however, the data collected showed larger discrepancies between the probes. To determine which probe was recording the correct specific conductance of the water, the continuous data from each logger was plotted with grab sample data from this location. The Blue SpC probe showed values closest to that of the grab samples collected, it should be noted that when these samples were collected their time was correlated to the closest 15-minute interval of the data loggers (Figure 14). With this stated, the samples are very close to that of the Blue probe but do show slight variations due to time differences

pH Reading Averages vs. Julian Date

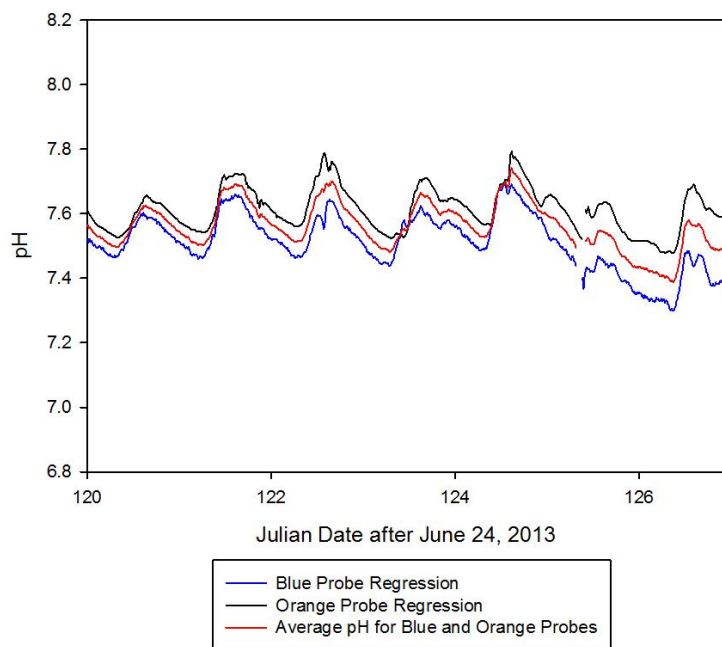


Figure 13- Average of Orange and Blue pH probes, Greensburg field site. Source: Compiled by the author.

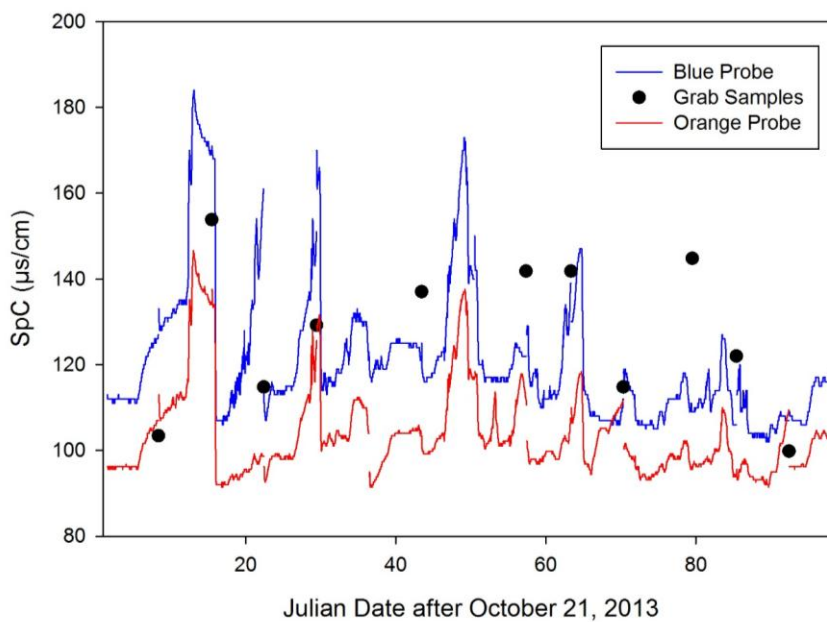


Figure 14- Continuous SpC from two Greensburg sondes with grab sample SpC data. Source: Compiled by the author.

and an approximate 150 m difference in river location (data logger site and USGS gauge/bridge site). Although a slight discrepancy was noted between these values, further investigation with a YSI 556 at the data logger site showed the Blue probe was in fact recording closer SpC data to the grab samples.

Discharge data for both sites were obtained at 15-minute intervals by means of the USGS gauging station (Munfordville, Kentucky) and stage data obtained through data logger recordings at the Greensburg site. Discharge data for Munfordville were directly obtained from the USGS National Water Information System Web Interface. The data were then aligned with that of the date and times for the field site data loggers. Several duplicate times/recordings were found in the discharge data from the USGS and these were deleted prior to adding these data to the master spreadsheet. The USGS gaging station at Greensburg, Kentucky does not record continuous discharge data; therefore, a rating curve was obtained from NOAA's National Weather Service Ohio River Forecast Center. A polynomial cubic regression was applied to the rating curve, resulting in the relationship

$$Q = -580.1 + 544.0 * x + -19.1 * x^2 + 1.4 * x^3 \quad (4)$$

Where Q is discharge in ft^3/s and x values are stage values in feet. Initially, this regression appeared to be the closest fit for this curve; however, at stages lower than 0.46 m (1.5 ft.) the regression deviated resulting in negative discharge values. To remedy this for these low stage levels a linear regression was applied for the lowest data points, resulting in the relationship

$$Q = -25.0 + 150.0 * x. \quad (5)$$

The data were then processed with an “if, then” structure, such that if the stage was above 0.46 m, then polynomial cubic regression was used, and if it was below this stage the equation reverted to the linear regression (Figure 15). It should be noted that the polynomial and linear equations used here were found to be the best fit for the data, multiple attempts were made using other equations but were not found to adequately represent the rating curve. Both the data obtained from the USGS and the equations used to transform the stage data at Greensburg to discharge data using the revised rating curve, was done so by converting between feet and meters. They are represented as both in this section.

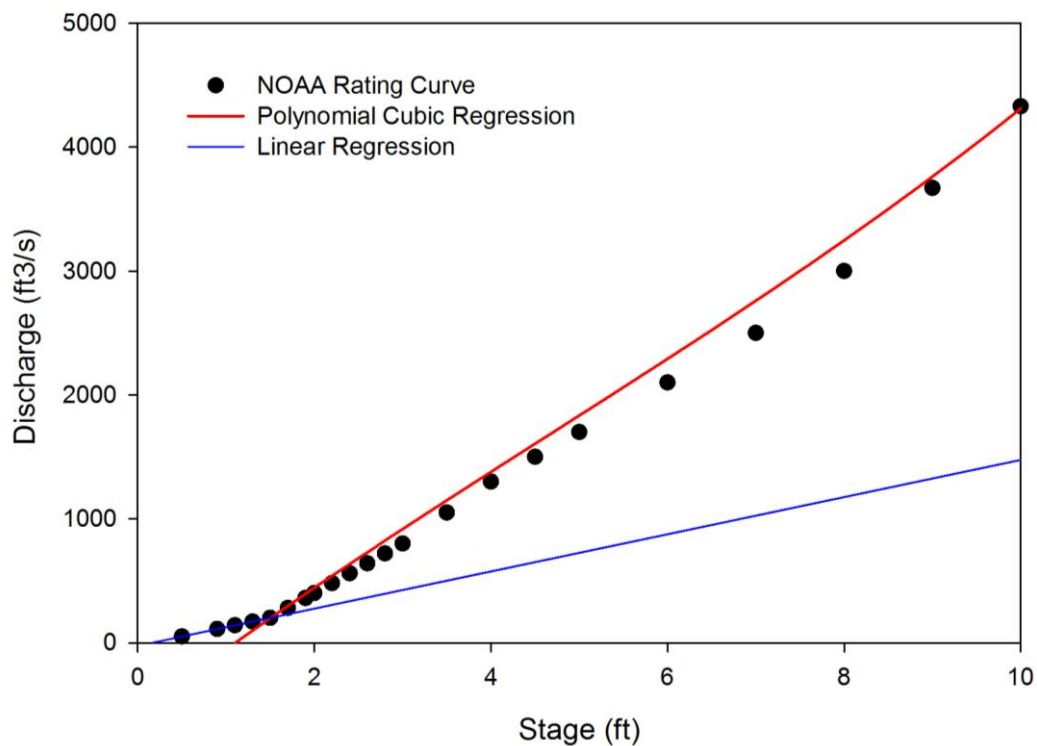


Figure 15- Rating Curve used for Greensburg Discharge. Source: Compiled by the author.

Data were also analyzed to determine relationships between SpC and various ions including HCO_3^- , Ca^{2+} and Mg^{2+} . This was accomplished through the regression of grab sample data with the YSI 556 for specific conductance, laboratory titrations for HCO_3^- , and analysis on the ICP for concentrations of Ca^{2+} and Mg^{2+} . Once post processing was complete on each of these variables to ensure that concentrations were correct, the data were imported into an Excel spreadsheet. This spreadsheet was designed to analyze for the mean value of bicarbonate for each water sample, as titrations were completed three times per sample each date had three samples for each location. Those values that had charge balance errors within 7% for the specified ions above were then used to determine relationships between SpC and these ions.

DIC and Carbon Flux

Prior to calculating the dissolved inorganic carbon (DIC), or carbon flux, the data were first processed and prepared for the calculations using Excel 2013 and Sigma Plot 11.0. This included determining the linear regressions for all ionic relationships to be utilized in those mass balance equations. All samples with a charge balance error of $> \pm 7\%$ in the equivalents equations were used and were not normalized. These processes included developing correlations between grab sample data for both Greensburg and Munfordville for HCO_3^- , Ca^{2+} , Mg^{2+} and SpC. The linear regressions produced were then applied to the 15-minute SpC data obtained from the data loggers deployed at the field sites, which resulted in a 15-minute temporal resolution for each of these ion. However, this high-resolution data were produced through the statistical relationship between the ions (Ca^{2+} and Mg^{2+}) and SpC, which had low R^2 values.

As a result of the weak relationships between these ions and SpC as reflected in their low R^2 values a data set reflecting actual measured values of these ions with weekly resolution was produced as an alternative to the high temporal resolution. This was accomplished by applying the grab sample concentration for each of these ions to the Julian Date both 3.5 days prior to the sample time collected as well as the subsequent 3.5 days. This 7-day period was chosen so as to give the best extrapolation of the riverine ionic concentrations, Ca^{2+} and Mg^{2+} , over this time period as the R^2 values proved to be weak; therefore, interpretations of these values for 15-minute resolution data were subject to additional error. Dissolved inorganic carbon and atmospheric carbon fluxes could then be calculated on both 15-minute intervals, as well as weekly intervals, using these ions in addition to pH, water temperature, and discharge for each watershed from October 21, 2013, through January 27, 2014 (Julian Dates after June 24, 2013, 118-216).

The dissolved inorganic carbon and atmospheric carbon flux were calculated for the watersheds through a series of mass balance calculations. Activities of CO_3^{2-} and $H_2CO_3^*$ were calculated using appropriate equilibria constants:

$$\{H_2CO_3^*\} = \frac{\{H^+\}\{HCO_3^-\}}{K_1} \quad (5)$$

and

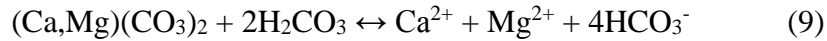
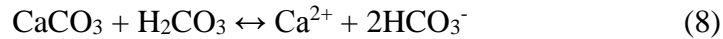
$$\{CO_3^{2-}\} = \frac{K_2\{HCO_3^-\}}{\{H^+\}} \quad (6)$$

where brackets denote species activities, $H_2CO_3^*$ is the sum of $H_2CO_3^*$ and aqueous CO_2 , and K_1 and K_2 are temperature dependent dissociation constants for carbonic acid (Harned

and Owen 1958; Stumm and Morgan 1996). Ion pairs and complexes were assumed to be negligible. These inorganic carbon species were then summed to obtain dissolved inorganic carbon (DIC) where

$$DIC = [CO_3^-] + [HCO_3^-] + [H_2CO_3^*]. \quad (7)$$

An estimate of the carbon sink from mineral weathering was obtained by considering the inorganic carbon products from the reactions:



For each two moles of inorganic carbon that result in each reaction, one came from the rock as $CaCO_3$ and the other came from the atmosphere as CO_2 gas dissolved in water forming H_2CO_3 (Groves et al. 2002). The atmospheric carbon source comes either directly as CO_2 gas from the atmosphere, or soil CO_2 gas from mineralization of organic carbon, primarily from decaying vegetation, as plants get this carbon from the atmosphere as well. Since this is true for both the end members calcite and dolomite, it is also the case for the range of various intermediate calcium/magnesium ratios present in the carbonate rocks of the upper Green River Basin. Thus, the atmospheric sink was measured by taking half of the total estimate of inorganic carbon flux (Amiotte-Suchet and Probst 1995). It has been suggested that the presence of strong acids in rainfall can potentially alter the ratio of atmospheric to mineral carbon produced as a consequence of details of the kinetics of limestone and dolostone dissolution (Groves and Meiman 2001, 2002). However, these

processes were not considered here because the effect was likely to be relatively small compared to the uncertainty in the DIC values based on the weak $\text{HCO}_3^-/\text{SpC}$ regressions, especially considering that the impacts of sulfuric acid deposition in the Upper Green River Basin rainfall have substantially diminished in the last five years with the most pH rainfall now over 5.0 [see: <http://nadp.isws.illinois.edu/nadp/>], following air quality improvements at regional coal burning facilities (Bob Carson, National Park Service, personal communication 2014).

Chapter 4: Results and Conclusion

The hydrochemistry and carbon flux of two nested watersheds within the Upper Green River Basin were studied for several months during the fall and winter of 2013 and 2014. This multi-parameter research consisted of 15-minute resolution data evaluating stage, pH, SpC, and water temperature with weekly grab samples collected for anions and cations. These data showed variations between the hydrogeology and geochemistry of the watersheds as well as seasonal deviations within each watershed.

Results of pH Data

Measurements for pH were obtained over a 99-day period for Greensburg and Munfordville where temporal and spatial variability was found between the watersheds. The pH values for these sites ranged from 7.0 – 8.0. With the exception of several days in October and again in November, the pH in Munfordville remained higher than that of the

pH in Greensburg (Figure 16). Munfordville saw pH fluctuations from 7.3 – 8.0, while those of Greensburg varied between 7.0 and 7.9. It was found that mean values for Munfordville and Greensburg were 7.7 and 7.4, respectively. Altogether, the range in pH was 0.74 and 0.88 pH units for Munfordville and Greensburg, respectively.

Seasonal variations in pH were observed between the warm months of early fall and colder winter months during the sampling period. Diel cycles were prominent during October; however, these diminished as the season progressed (Figure 17). A two-week period in both the fall and winter were examined more closely, October 21-November 4, 2013 and January 1-14, 2014 (Julian Dates 1-14 and 72-86, respectively). When compared (Figure 17), these periods show distinct dissimilarities in diel-scale changes.

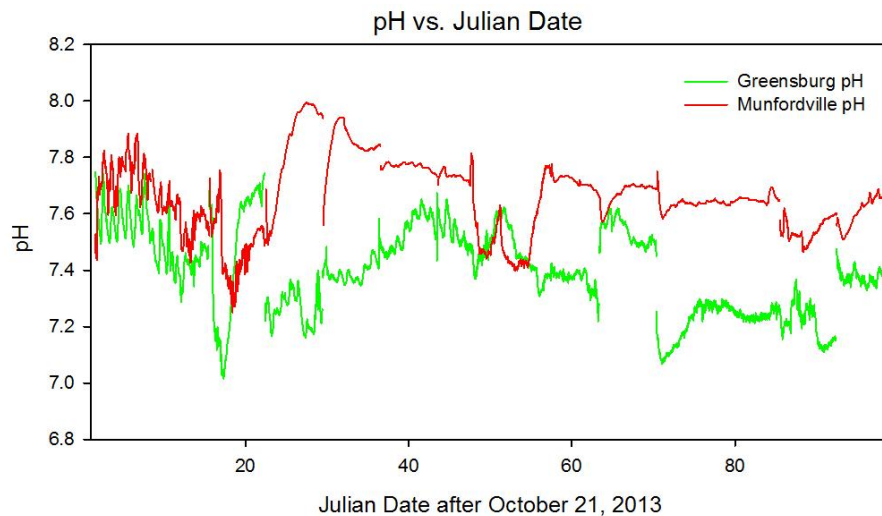


Figure 16- Graph of pH values for Greensburg and Munfordville. Source: Compiled by the author,

Both field sites show the presence of diel cycles through the warm early fall sampling. The last week in October depicts almost symmetrical rises and falls in pH for Greensburg, approximately 0.2 pH units per day, with the continuation of these cycles

into the beginning of November, but with less intensity. Munfordville also followed this pattern; however, more noise was observed indicating additional small variations in pH as it changed over 24-hour cycles. These diel cycles were not detected during colder temperatures, as shown through the January 1-14 time period. This period was marked by very limited shifts in pH values for both sites, only fluctuating approximately 0.2 pH units over the entire two week period, with the largest changes occurring over January 13 and 14. The very small fluctuations mentioned for Munfordville during the fall were observed in the Greensburg data over this colder period. The oscillation in pH data for these sites was an indicator of changes due to seasonality, as well as the hydrochemical differences between the watersheds. Figure 18 depicts the differences between pH for the two sites where those values above zero represent higher Munfordville pH values and those below the zero threshold indicate higher pH values for Greensburg. Although there was an error range of ± 0.2 for the pH probes, < 90% of the recordings showed higher pH values for the Munfordville site, indicating a definite pH variance between the locations.

pH vs. Julian Date, Two Weeks- Falls and Winter 2013/2014

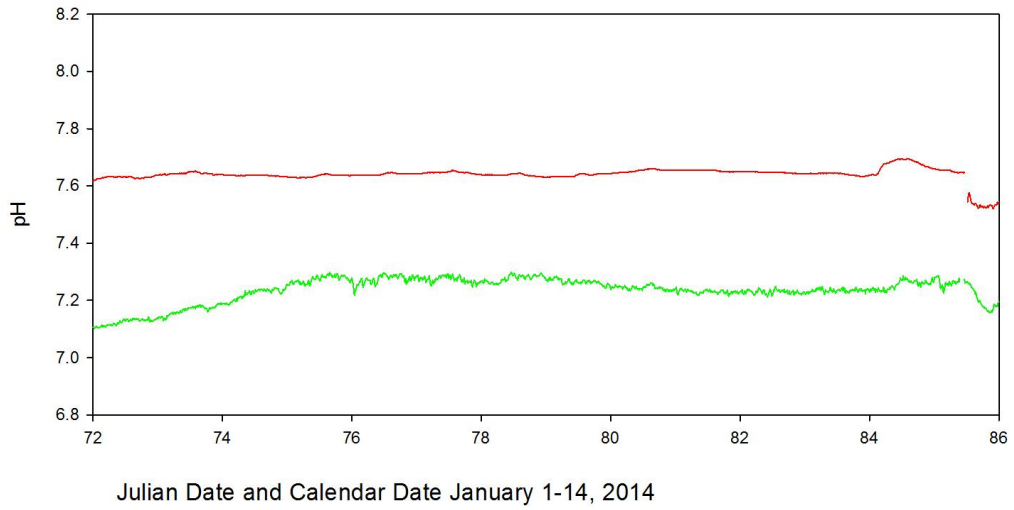
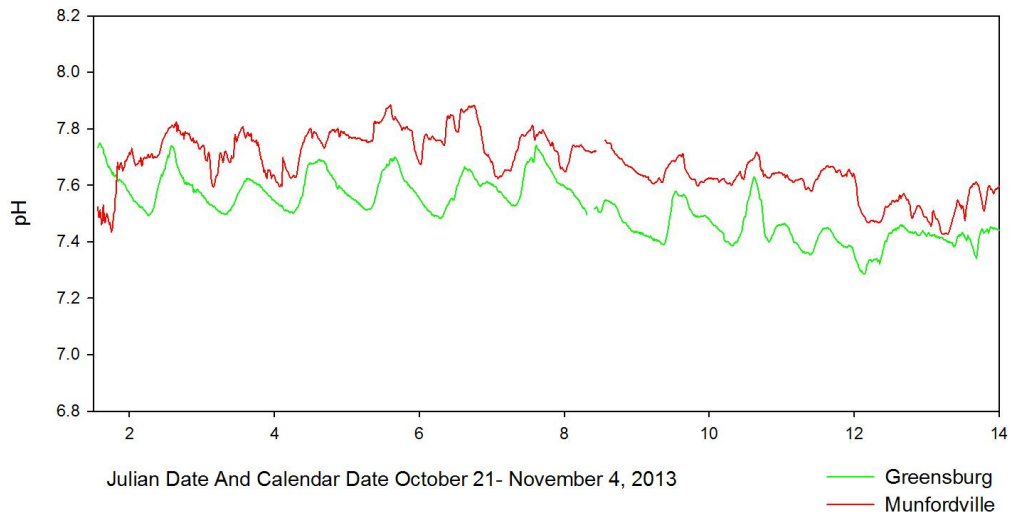


Figure 17- Graphs of warm and cold period pH variations, Greensburg and Munfordville, KY. Source: Compiled by the author.

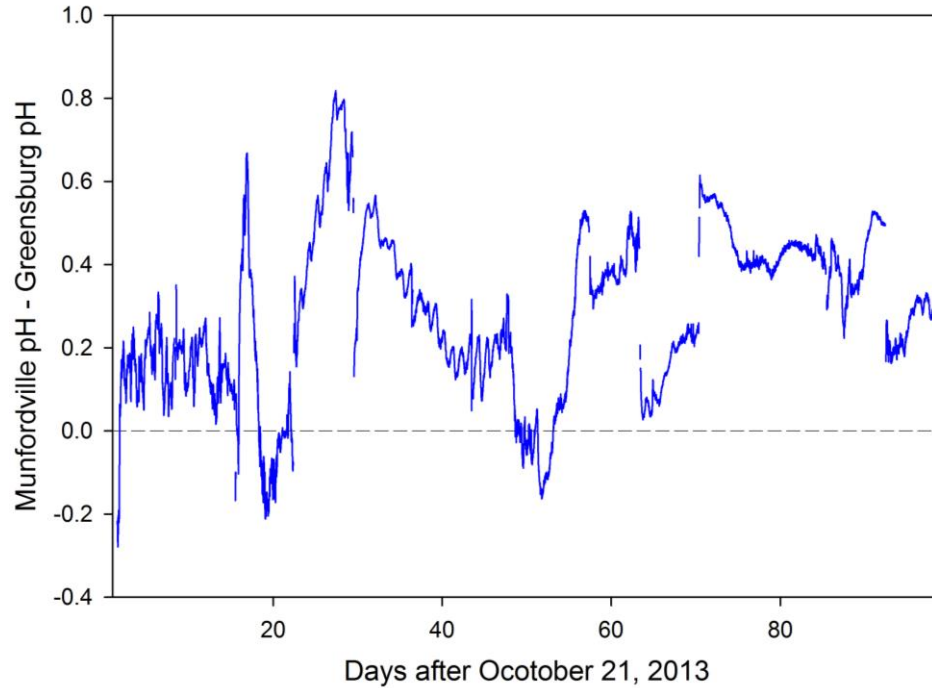


Figure 18- Difference in watershed pH, Munfordville – Greensburg. Source: Compiled by the author.

Results of SpC Data

The specific conductance (SpC) was found to be considerably different at the field sites. The data logger placed in Munfordville consistently recorded higher SpC values than those observed in Greensburg (Figure 19). This is most clearly signified by the fact that there were only two overlapping data points between the sites, which occurred on November 9, 2013. Although both sites experienced fairly regular increases and decreases in spC, by comparison Munfordville was subject to typically larger spikes in specific conductance followed by sharp decreases. In contrast, typically Greensburg saw rapid spikes in SpC, but at differing magnitudes than those seen in Munfordville.

The range for Munfordville extended from 125-344 $\mu\text{s}/\text{cm}$ while that of Greensburg was only 102-184 $\mu\text{s}/\text{cm}$. This indicated that over the 99 day period, the Munfordville site not only averaged a mean of 119 $\mu\text{s}/\text{cm}$ higher than that of Greensburg (239. $\mu\text{s}/\text{cm}$ to 120 $\mu\text{s}/\text{cm}$), but that site's range extended 127 $\mu\text{s}/\text{cm}$ further than that of Greensburg. The differences in specific conductance between the sites is most notable during colder conditions. Under these conditions, spC nearly plateaued in Greensburg while the spikes in Munfordville are more intense than those detected in earlier months (Figure 19). Figure 20 shows the ratio of spC for the field sites. This graph clearly depicts the higher spC values for the Munfordville watershed as on only one occasion does spC for the Munfordville field site dip below that of Greensburg.

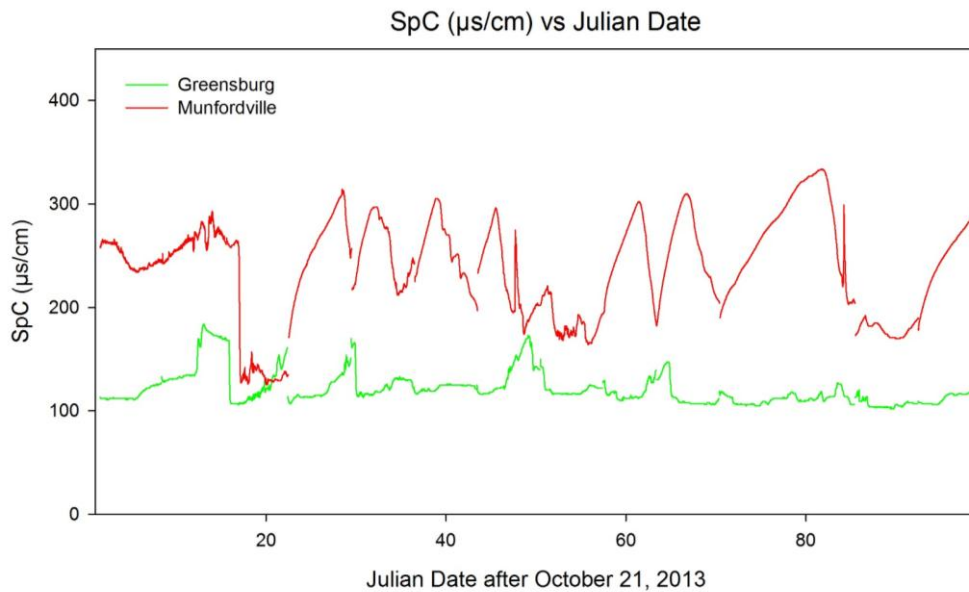


Figure 19- Graph of SpC for Greensburg and Munfordville. Source: Compiled by the author.

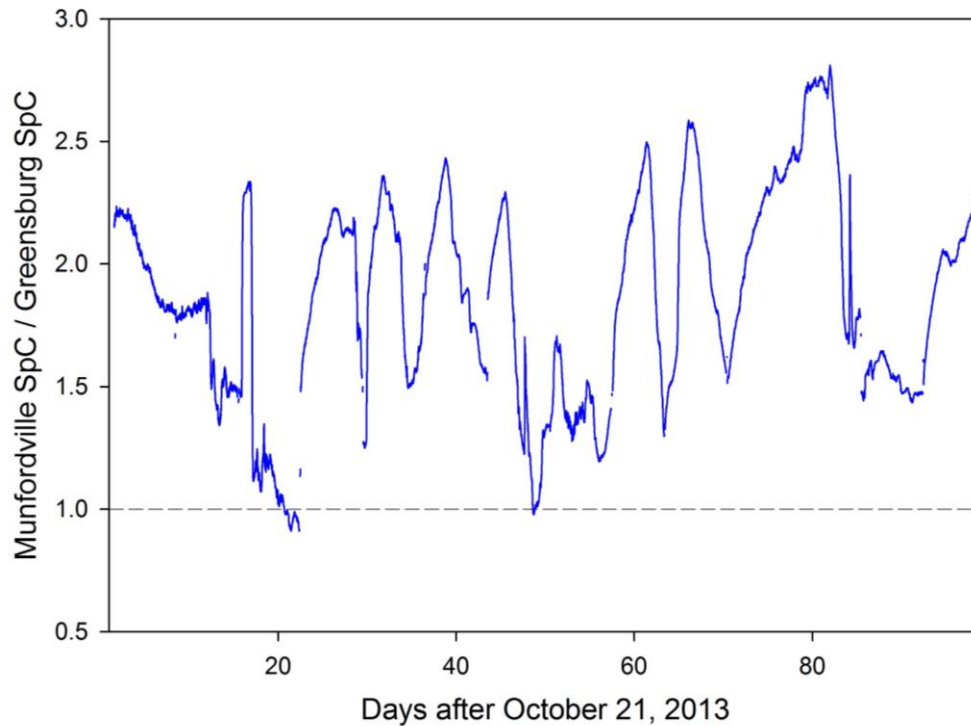


Figure 20- Ratio of Munfordville and Greensburg specific conductance. Source: Compiled by the author.

Results of Water Temperature Data

Water temperature data were also collected on 15-minute intervals from October 2013 to January 2014. Temperatures progressively declined throughout this period; nevertheless, with these these overarching temperature reductions, shorter scale fluctuations also occurred (Figure 21). The maximum water temperature recorded was 16.7 °C in Greensburg with a maximum for Munfordville of 15.2 °C. The lowest temperatures reached were -0.1 °C and 0.6 °C for Greensburg and Munfordville, respectively. The mean water temperatures for the field sites were very similar, 8.7 °C for Greensburg and 8.2 °C for Munfordville. Observations of seasonal data showed some degree of consistency in

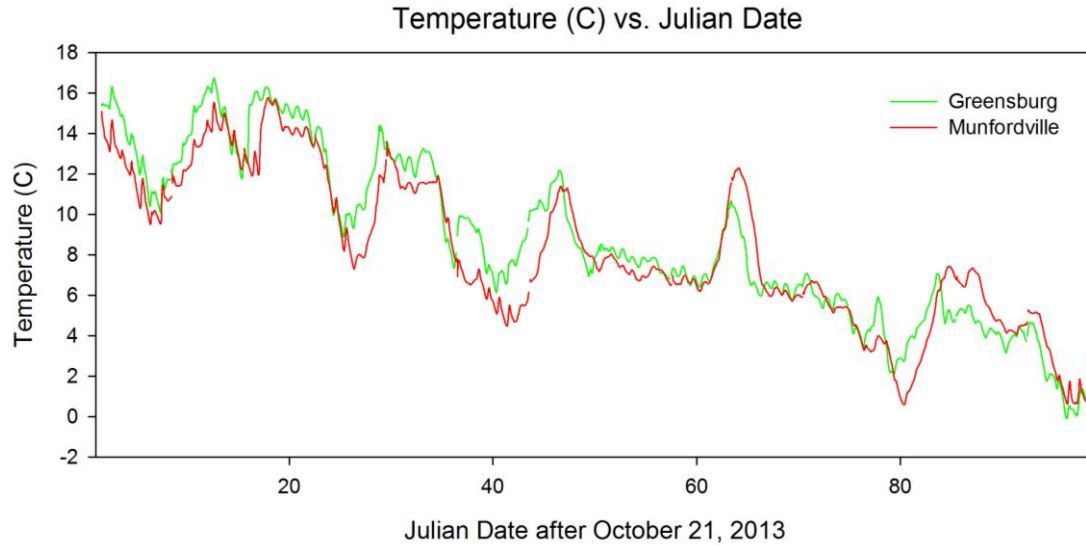


Figure 21- Graph of Temperature vs. Julian Date after October 21, 2013. Source: Compiled by the author.

diurnal temperature fluctuations during the fall, October 21, 2013 – November 4, 2014. Diurnal temperature variations were not as distinct during the colder months, though they were slightly more pronounced in Greensburg than Munfordville (Figure 22). Water temperatures at both sites had an overall cooling trend over the entire sampling period, although it was found that Greensburg had generally warmer water temperatures during the warmer months while Munfordville showed warmer temperatures during the cooler months (Figure 23).

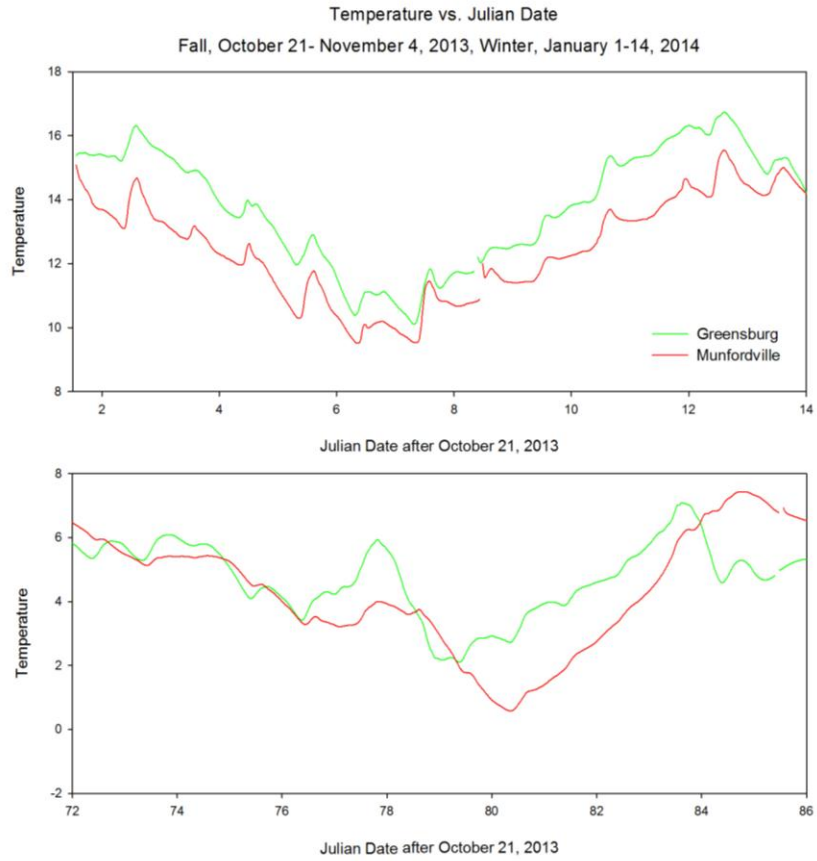


Figure 22- Graph of Temperature vs. Julian Date after October 21, 2013. Source: Compiled by the author.

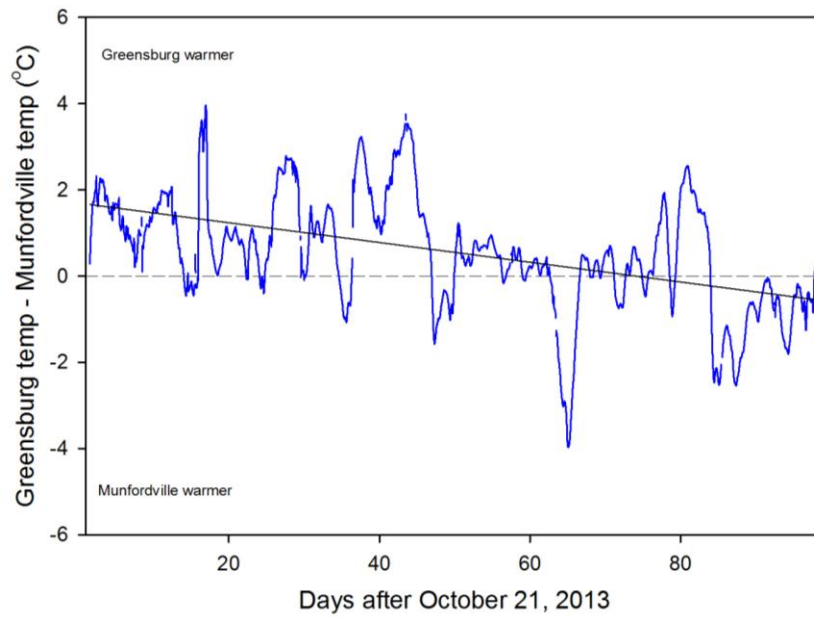


Figure 23- Difference in field site water temperature. Source: Compiled by the author.

Results for Discharge Data

The discharge along this reach of the Green River varies greatly, as it ranged from approximately 178,000 l/s in Greensburg to 427,000 l/s in Munfordville over the study period. As expected, all discharges for the downstream site remained greater than that of the upstream field site (1,310 and 179,627 l/s and 9,061 and 436,075 l/s, for minimum and maximum discharges for Greensburg and Munfordville respectively). These larger maximum and minimum values were indicative of the overall discharge for the reach, as there were very few time periods in which the Munfordville discharge was recorded to be lower than that of Greensburg (Figure 24). The increased discharge along the 50 km reach can be attributed to inputs from releases from the dam (which also effects the Greensburg site), surficial tributary streams, springs, and runoff, in addition to throughflow and baseflow.

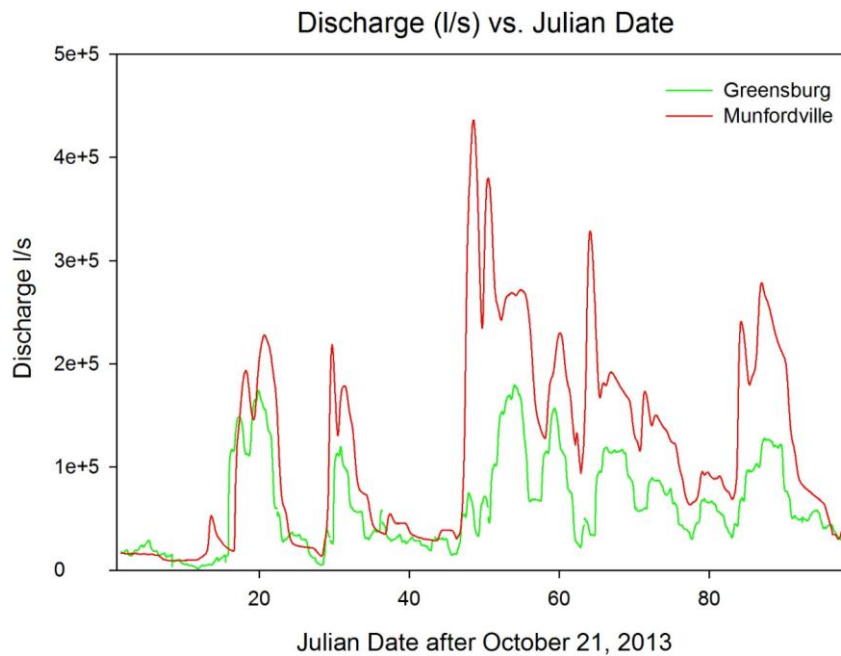


Figure 24- Graph of Discharge l/s for field sites. Source: Compiled by the author.

Relationships in Hydrochemistry

Discharge and SpC are closely related, with specific conductance commonly acting inversely to the rise and fall of discharge along the reach. The SpC for Greensburg and Munfordville both showed these responses in relation to discharge, often occurring simultaneously. Rapid increases in discharge and decreases in SpC transpired sharply over several hours, these are represented by the linear variations in Figures 25 and 26. The rebound for SpC was found to be slower than the initial response to the influx of discharge at Greensburg. In addition, smaller discharge events were marked by gradual decreases in SpC, which recovered with the decrease in water levels. SpC readings in Munfordville reflected a much more erratic relationship with discharge resulting in fewer gradual increases or decreases in SpC. The data loggers at this site recorded escalations and declines of greater magnitude than that observed at Greensburg. As a result, the river in Munfordville showed almost constant and greatly varying changes in SpC, and while Greensburg also had periods of increased fluctuation, there were also extended periods of plateaued levels.

The pH and SpC conditions were compared to determine relationships for the individual sites in addition to hydrochemical differences between the sites. Analysis of these parameters for Greensburg showed pH reflecting nearly all the peaks and troughs in SpC, with Munfordville also sharing this relationship, but not to the same extent. The pH and SpC both predominantly rose and fell in unison. Julian Dates 32-43 showed periods of rapid SpC fluctuation with little to no change in pH, while Greensburg recorded a steady increase then decrease for pH with a matching gradual rise then fall in SpC (Figures 27 and 28).

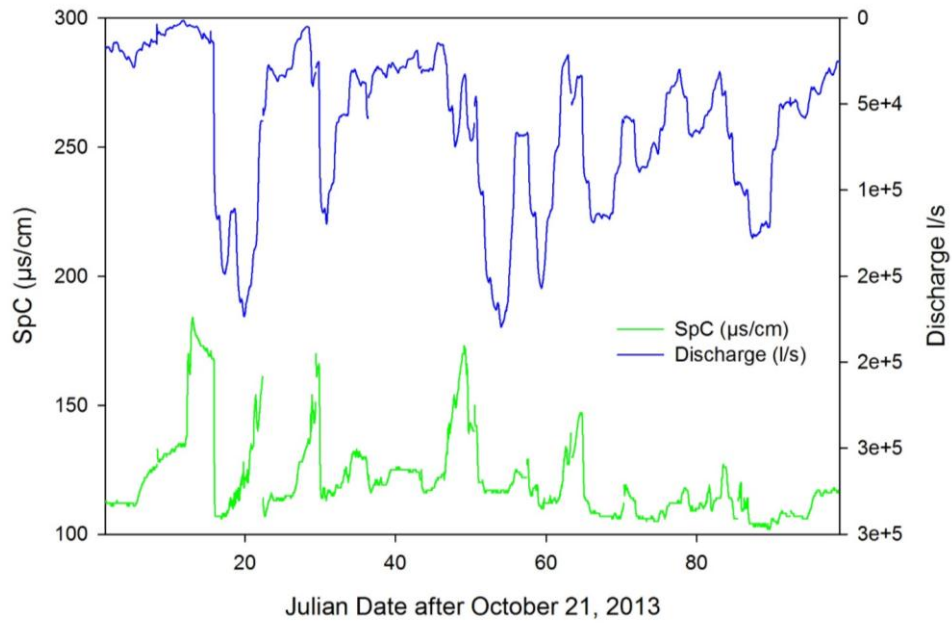


Figure 25- Graph of SpC and Discharge, Greensburg.

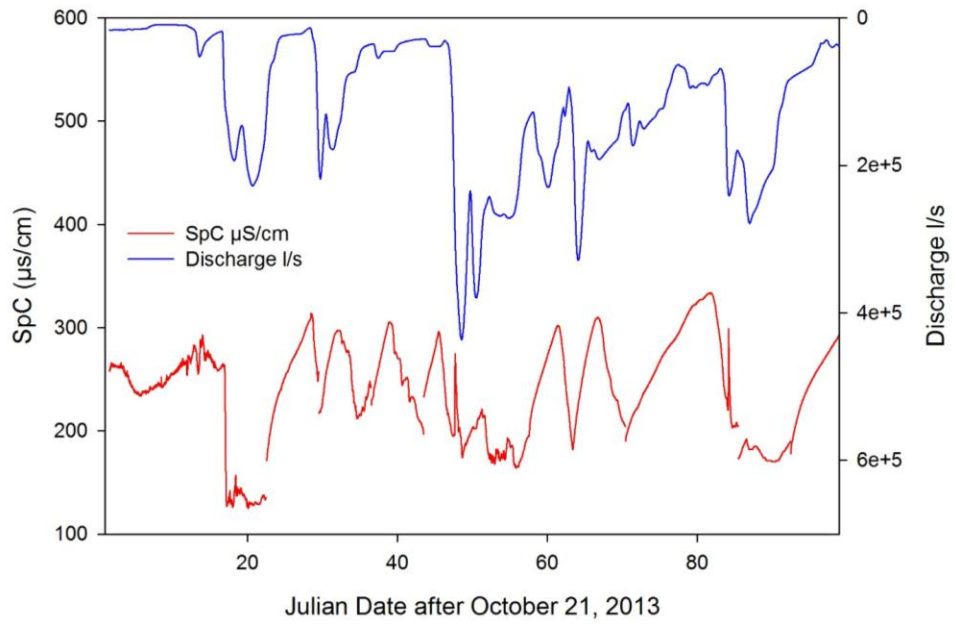


Figure 26- Graph of SpC and Discharge, Munfordville. Source: Compiled by the author.

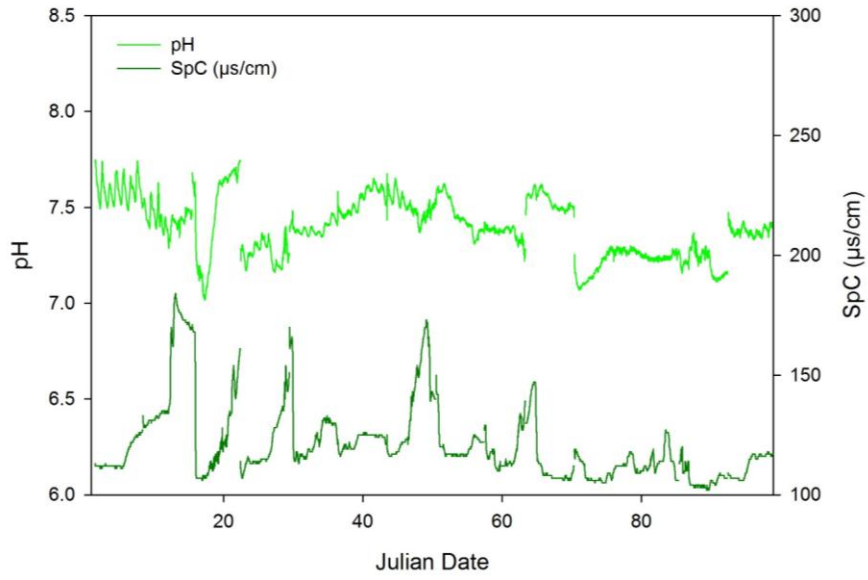


Figure 27- Graph of pH and SpC, Greensburg.

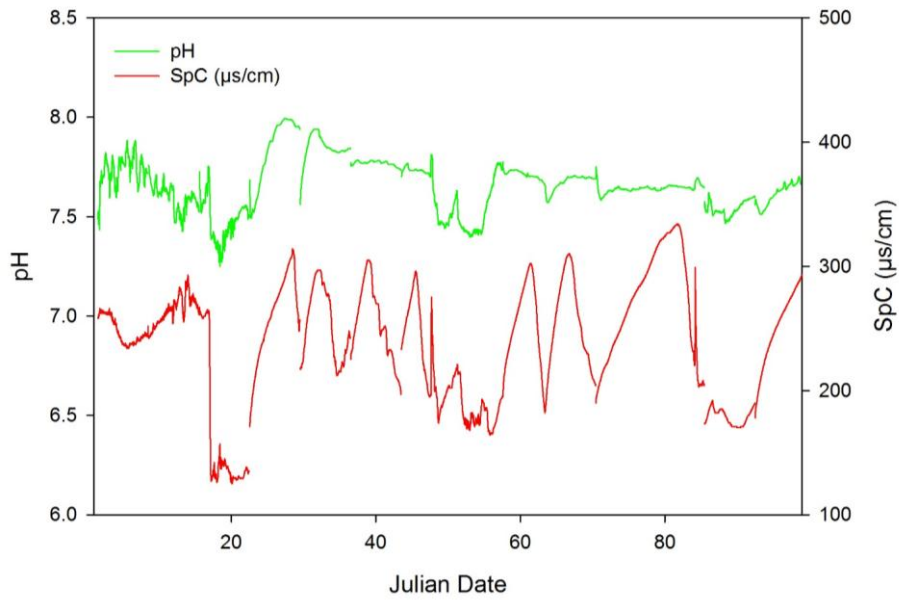


Figure 28- Graph pH and SpC, Munfordville. Source: Compiled by the author.

Ionic Relationships

To determine how closely the HCO_3^- and SpC data were related, grab sample data for both parameters were plotted together. This process was implemented for the determination of all ionic relationships with specific conductance. The R^2 value was then determined to measure how closely these data were associated, which resulted in a percentage of the variable variation explained by the linear model. The closer the R^2 value was to 1.0 the closer the relationship between the compared variables. With respect to HCO_3^- and SpC, R^2 values were found to be 0.24 and 0.32 for Greensburg and Munfordville, respectively (Figures 29 and 30).

These methods were also employed to determine relationships between SpC and Ca^{2+} and SpC and Mg^{2+} . The linear equations utilized for these purposes resulted in very low R^2 values for these parameters. Correlations for Greensburg were found to be 0.03 for Ca^{2+} and SpC and 0.004 for Mg^{2+} and SpC (Figures 31 and 33). Although R^2 values for Munfordville were still very low the relationships between these parameters did show some improvement from the upstream sites with values of 0.12 and .023 for Ca^{2+} and SpC and Mg^{2+} and SpC, respectively (Figures 32 and 34). The most notable difference was the improved relationship between these ion species and specific conductance as they moved downstream through a largely homogenous watershed dominated by carbonate bedrock, although the presence of ions from sources other than rock dissolution in both cases meant that the SpC was of nearly no predictive value. Fortunately in the calculations for DIC and the atmospheric carbon flux the calcium and magnesium values are used only indirectly to determine ionic strength in the activity corrections, and thus these errors have minimal impact on the carbon sink and DIC values.

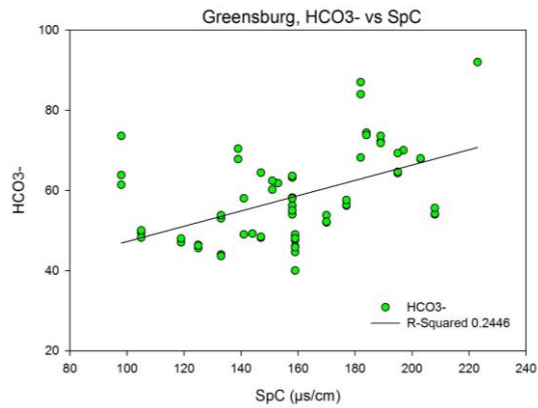


Figure 29- HCO_3^- and SpC , Greensburg.

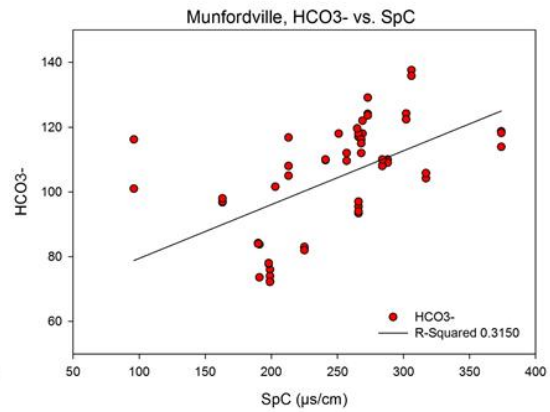


Figure 30- HCO_3^- and SpC , Munfordville.

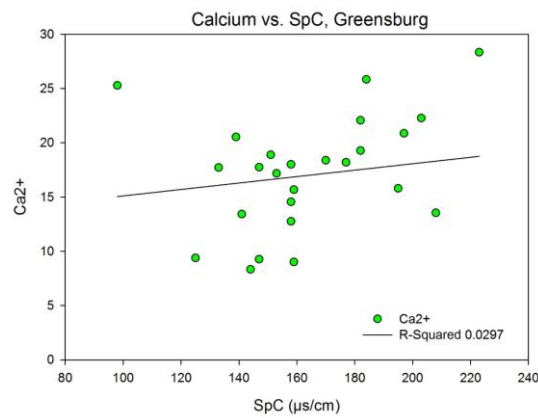


Figure 31- Ca^{2+} vs SpC , Greensburg.

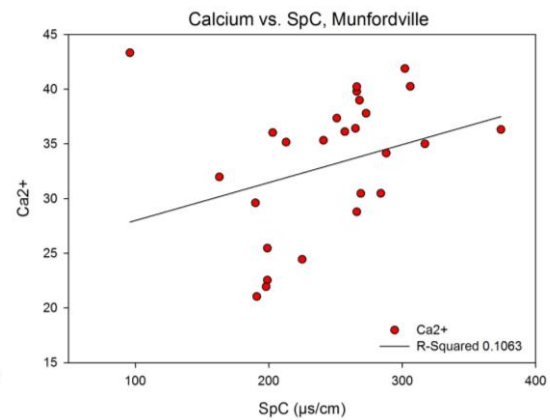


Figure 32- Ca^{2+} vs SpC , Munfordville.

Source: Compiled by the author.

Dissolved Inorganic Carbon

The relationships between ions utilized for mass balance equations needed for DIC and atmospheric carbon flux were found to have low R^2 values, as previously discussed (HCO_3^- and SpC in direct calculations, Ca^{2+} and SpC , Mg^{2+} and SpC used

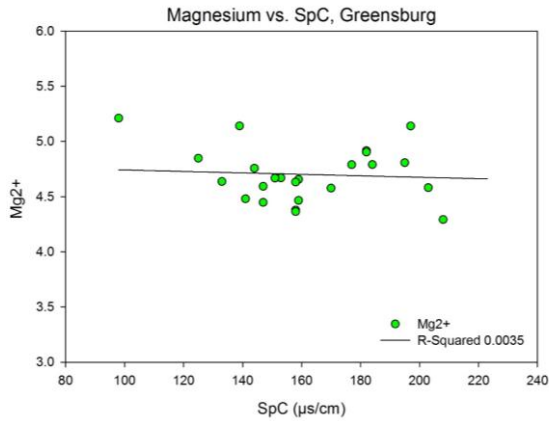


Figure 33- Mg^{2+} vs SpC, Greensburg.

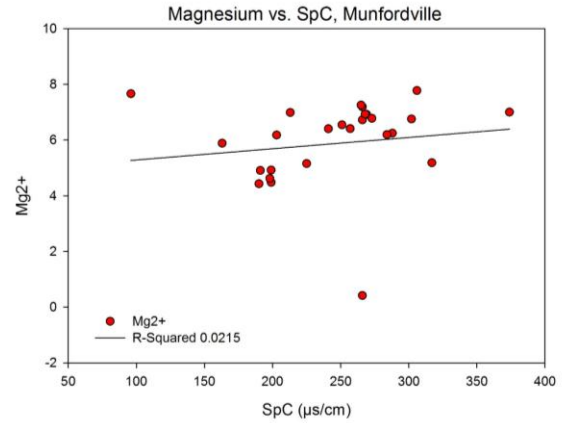


Figure 34- Mg^{2+} vs SpC, Munfordville.

Source: Compiled by the author.

indirectly). As a result, utilizing the linear regressions from these relationships was subject to uncertainty, therefore calculations for DIC and carbon flux were processed using both 15-minute resolution, with these regressions, and a coarser weekly resolution utilizing grab sample data for these ions extended 3.5 days pre- and post-sampling. Early research methods in studies that utilized direct sampling of water chemistry, such as in landscape denudation studies, prior to the availability of data loggers, used approaches similar to the latter method described. This research, however, built upon those methods to use not only the weekly ionic grab sample data, but also 15-minute resolution data for pH, water temperature, and discharge. As a result these coarser methods were improved upon by newer technologies in an event where linear statistical relationships proved to be susceptible to uncertainty. The results of mass balance equations utilizing statistical relationships between Ca^{2+} and SpC and Mg^{2+} and SpC as well as weekly data and 0 values for these parameters are as follows (note the entire result is displayed for comparison),

	Units- ($\text{gkm}^{-2} \text{d}^{-1}$)		15-minute Resolution
Greensburg	Atmospheric Flux	With Ca^{2+} and Mg^{2+} regression values	263434489
	DIC	With Ca^{2+} and Mg^{2+} regression values	526868978
	Atmospheric Flux	0 value for Ca^{2+} and Mg^{2+}	268810469
	DIC	0 value for Ca^{2+} and Mg^{2+}	537620939
	Atmospheric Flux	Weekly Data Values for Ca^{2+} and Mg^{2+}	263163477
	DIC	Weekly Data Values for Ca^{2+} and Mg^{2+}	526326954
Munfordville	Atmospheric Flux	With Ca^{2+} and Mg^{2+} regression values	229677634
	DIC	With Ca^{2+} and Mg^{2+} regression values	459355268
	Atmospheric Flux	0 value for Ca^{2+} and Mg^{2+}	235569409
	DIC	0 value for Ca^{2+} and Mg^{2+}	471138819
	Atmospheric Flux	Weekly Data Values for Ca^{2+} and Mg^{2+}	229974385
	DIC	Weekly Data Values for Ca^{2+} and Mg^{2+}	459948770

Figure 35- Table of differences in 15-minute resolution data. Source: Compiled by the author

Differences were found in the results from both the 15-minute and weekly calculations; however, the results of both resolutions between the upstream and downstream watersheds showed good agreement for comparable measurements. Area and time normalized (meaning normalized by the carbonate bedrock in each watershed and by the time per day) atmospheric carbon sink measurements ($\text{gkm}^{-2} \text{d}^{-1}$) for Greensburg with 15-minute data agreed with those from Munfordville within 12%, and for weekly resolution data within 33%. The results were as follows:

Units- ($\text{gkm}^{-2} \text{d}^{-1}$)		Weekly Resolution	15-minute Resolution
Greensburg	Atmospheric Flux	3.3×10^8	2.6×10^8
	DIC	6.5×10^8	5.3×10^8
Munfordville	Atmospheric Flux	2.3×10^8	2.2×10^8
	DIC	4.6×10^8	4.4×10^8

Figure 36- Atmospheric carbon flux and DIC results for Greensburg and Munfordville watersheds. Source: Compiled by the author.

The use of data on a 15-minute or weekly resolution had minimal impact on the results for Munfordville, although the use of these resolutions played a larger role in the calculations for atmospheric carbon flux and DIC Greensburg.

Conclusion

Carbon flux research along a 50 km reach of the Upper Green River Basin provides insight into dissolved inorganic carbon and atmospheric carbon fluxes in a karst influenced, surficial riverine environment in both heterogeneous and predominantly homogenous carbonate watersheds. Hydrogeochemical differences were observed with relation to pH, SpC, water temperature, and discharge, although comparison of area and time normalized carbon sink and DIC flux estimates showed good agreement through percent error comparison.

Higher pH values downstream of Greensburg were attributed to a more buffered system from amplified dissolution of carbonate bedrock as a result of increasingly homogenous and purer limestone (Dicken 1935). These dissolution processes were

measurably higher with increases in H^+ activity as H_2CO_3 interacted with exposed limestone ($CaCO_3$) shown through higher pH values recorded with at Munfordville. Although dissolution processes were occurring in the upstream watershed as well, as karst is also present there, these were not of the same magnitude, and this resulted in more subdued H^+ activities. In addition, the downstream site was also subjected to influxes of groundwater from springs along its journey, which flowed through the carbonate formations and was potentially subjected to increased dissolution due to its amplified exposure to the bedrock. Sampling at these locations (tributaries between the Greensburg and Munfordville field sites) was not within the parameters of this research, however previous literature has shown that karst groundwater has been found in general to have higher pH ranges (Katz et al. 1997; Hatcher 2013).

Lithological influences played a role in ionic distributions within this reach of the Upper Green River. Observations also showed distinct increases in SpC between the watersheds. As specific conductance is a measure of water's ability to conduct electricity across a distance at a given temperature, the more ions present in the sample the higher the specific conductivity. This was clearly observed in the Munfordville data set, as only once during the sampling period did this site record readings as low as those present at the upstream site. This indicates that not only were increased karst dissolution processes adding to the dissolved constituents in the water, but other potential sources along the river's path were contributing as well. These potential sources included overland flow and additional tributaries. Anthropogenic impacts also have influences on ionic concentrations; a considerable portion of these watersheds is utilized for agricultural purposes, therefore the increase in SpC in the lower reaches can also be attributed to influxes from these

activities. Examples of such increases in ionic concentrations from potential agricultural influences include potassium, nitrates, and phosphates, which were measured in higher concentrations in many of the samples. These higher concentrations are often indicative of agricultural activities (Mehnert et al. 2005; Moore et al. 2009).

The influence of discharge on SpC is also notable and the inverse relationship can be credited to dilution factors during large influxes of water; however, in contrast when water levels were at or near base flow, higher concentrations were recorded indicating more ionic activity. During these high flow events, additional ions would be added to the system through additional pathways (runoff and rainfall); however, the large amounts of water being contributed would diminish the conductivity between them as discharge increases. During high discharge events increased dissolution occurs as aggressive water flows over exposed bedrock, increasing the ionic constituents in the river (Palmer 2007) raising the SpC measurements. However, the data have shown that the influx of water into the system, during high discharge events, overshadow the ionic loading causing this inverse relationship.

Discharge differences between the sites were observed with Munfordville showing higher recordings than that of Greensburg, as would be expected, attributed to additional surface and subsurface influxes to the river system. These channels likely play an important role in varying water temperatures between the field sites. The upstream site showed predominantly warmer water temperatures through the fall and early winter of 2013; however, recordings in January, 2014, showed a reversal in this trend with Munfordville data loggers recording higher temperatures. As this site was subjected to influxes of groundwater from upstream springs, downstream of Greensburg, this likely caused the

switch in previously observed temperature trends. O'Driscoll and Dewalle (2006) discussed meteorological influences having a greater impact on water temperature with increasing distance from springs. As is the case in Munfordville, several large springs feed into the river system upstream from this location, which have shown through this research to impact water temperatures at this location, whereas meteorological influences play the largest role on water temperatures for the Greensburg field site in conjunction with releases from the Greensburg dam, where water temperatures are influenced by the influx of water from these releases do to the close proximity to the dam and the water temperatures have had limited time to equilibrate.

Atmospheric carbon flux and dissolved inorganic carbon flux were measured for the two field sites, subsequently based upon regressions for the ionic relationships between SpC and HCO_3^- , and 15-minute resolution data; therefore, we also calculated these measurements based upon a coarser, weekly resolution (Perrin et al. 2008). Even with the relatively weak correlation between SpC and HCO_3^- used directly in the calculation, and between SpC and calcium, along with SpC and magnesium, respectively (used indirectly with minimal impact on results). Area and time normalized atmospheric carbon sink fluxes and DIC fluxes agree well between the two sites, within 12% for the 15-minute data and 33% for the weekly resolution data. This can be attributed to the fact that it has been shown in other locations (Groves and Meiman 2005; Cheng et al. 2011; White 2013) that solute fluxes in karst systems are more sensitive to discharge than concentration variations. Cai et al. (2008) also found that the total flux still amplified even while concentrations of HCO_3^- decreased during periods of higher discharge.

The atmospheric carbon flux for the upstream watershed was found to be 2.6×10^8 and $3.3 \times 10^8 \text{ gkm}^{-2} \text{ d}^{-1}$, while that of the downstream was calculated at 2.3×10^8 and $2.2 \times 10^8 \text{ gkm}^{-2} \text{ d}^{-1}$ (15-minute then weekly resolution). DIC also resulted in values very close for both methods used in the calculations, 5.3×10^8 and $6.5 \times 10^8 \text{ gkm}^{-2} \text{ d}^{-1}$ for 15-minute and weekly resolutions, respectively, for Greensburg, and 4.6×10^8 (15-minute) and $4.4 \text{ gkm}^{-2} \text{ d}^{-1}$ (weekly) for Munfordville. The results for atmospheric carbon flux and dissolved inorganic flux were normalized by the carbonate bedrock within each basin, these basins differed only minimally lithologically (although the Munfordville basin maintains much larger quantities of the lithologic variations); however, the Munfordville basin is much greater in size than that of Greensburg. The differences between these results can be attributed to noise within the data due to differences in resolution; however, for the purpose of analyzing these methods the data are very close and either set could be used for atmospheric carbon or DIC fluxes within the watersheds. Noise within the data due to resolution differences was attributed to 15-minute data for pH, SpC and weekly resolution for cations and anions, this could have resulted in minimal variances in ionic concentrations due to the extrapolation of grab sample data over the weekly time period.

Carbonate karst environments may play an intricate role in the sequestration of CO_2 (Liu et al. 2008). The connection between CO_2 , H_2O , and HCO_3^- in these environments is related to the global carbon budget (Liu and Zhao 2000). Investigations into the impacts of carbonate karst as a carbon sink and partitioning within this system on a local level is vital to understanding the global carbon cycle. International research has provided thorough scientific data regarding many aspects of these environments; however, additional investigations are needed to have a more comprehensive understanding of the inorganic

carbon partitioning within these systems. Gaps in the literature involving inorganic carbon flux in fluvial karst environments were addressed through high-resolution data collection on the Upper Green River. As society pushes for answers to climate change adaptation and mitigation, there will be increased opportunities for research in these areas. Having an in depth grasp on carbon sources, sinks, and partitioning on a local scale will provide a base level to understanding the global carbon flux and how best to move forward and plan for the future.

REFERENCES

- Amiotte-Suchet, P., Probst, J., 1995. A Global Model for Present-Day Atmospheric/ Soil CO₂ Consumption by Chemical Erosion of Continental Rocks (GEM-CO₂). *Tellus* 47B: 273-280.
- Amiotte-Suchet, P., Probst, J., Ludwig, W., 2003. Worldwide Distribution of Continental Rock Lithology: Implications for the Atmospheric/Soil CO₂ Uptake by Continental Weathering and Alkalinity River Transport to the Oceans. *Global Biogeochemical Cycles*, 17: 1038-1050.
- Anthony, D.M., Groves, C., Meiman, J., 2003. Preliminary Investigations of Seasonal Changes in the Geochemical Evolution of the Logsdon River, Mammoth Cave, Kentucky. *Speleogenesis and Evolution of Karst Aquifers*, 1(4): 1-6.
- Anthony, D.M., Groves, C., Meiman, J., 1998. Preliminary Investigations of Seasonal Changes in the Geochemical Evolution of the Logsdon River, Mammoth Cave, Kentucky: Speleogenesis and Evolution of Karst Aquifers. *The Virtual Scientific Journal*, 1(4): 1-6.
- Cai, W. J., Guo, X., Chen, C. T., Dai, M., Zhang, L., Zhai, W., Lohrenz, S. E., Yin, K., Harrison, P. J., Wang, Y., 2008. A Comparative Overview of Weathering Intensity and HCO₃⁻ Flux in the World's Major Rivers with Emphasis on the Changjiang, Huanghe, Zhujiang (Pearl) and Mississippi Rivers. *Continental Shelf Research*, 28: 1538-1549.
- Cao, J., Yuan, D., Groves, C., Huang, F., Yang, H., Lu, Q., 2012. Carbon Fluxes and Sinks: the Consumption of Atmospheric and Soil CO₂ by Carbonate Rock Dissolution. *Acta Geological Sinica (English Edition)*, 86(4): 963-972.
- Cheng, Z., Min, Z., Rui, Y., Zaihua, L., Gremaud, V., Goldscheider, N., 2011. Comparison of Karst Process-Related Carbon Sink Intensity Between an Alpine Glaciated and Snow Covered Karst Water System and Humid Subtropical Karst Water System. *Advances in Climate Change Research*, 3. Online at: http://en.cnki.com.cn/Article_en/CJFDTOTAL-QHBH201103004.htm
- Ciais, P., Borges, A. V., Abril, G., Meybeck, M., Folberth, G., Hauglustaine, D., Janssens, I.A., 2008. The Impact Of Lateral Carbon Fluxes on the European Carbon Balance. *Biogeosciences*, 50: 1259-1271.
- Cox, P. M., Betts, R. A., Jones, C. D., Spall, S. A., Totterdell, I. J., 2000. Acceleration Of Global Warming Due To Carbon-Cycle Feedbacks In A Coupled Climate Model. *Nature*, 408: 184-187.
- Crocker, H.B., 1992. *Green River*, In Kleber, J.E., Clark, T.D., Harrison, I.H., Klotter, J.C. (eds.) *The Kentucky Encyclopedia*. Lexington, KY: The University Press of Kentucky, 387-388.

- Currens, J.C., Ray, J. A., 1998. *Mapped Karst Groundwater Basins in the Somerset 30 x 60 Minute Quadrangle*, Ser. 11, Map and Chart 16, Scale 1:10,000. Lexington, KY: Kentucky Geological Survey.
- Currens, J.C., Paylor, R.A., Ray, J.A., 2002. *Mapped Karst Groundwater Basins in the Lexington 30 x 60 Minute Quadrangle*, Ser. 12, Map and Chart 35, Scale 1:100,000. Lexington, KY: Kentucky Geological Survey.
- Dicken, S.N., 1935. Kentucky Karst Landscapes. *The Journal of Geology*, 43(7): 708-728.
- Doctor, D.H., Alexander Jr., E.C., 2005. *Interpretation of Water Chemistry and Stable Isotope Data from a Karst Aquifer According to Flow Regimes Identified through Hydrograph Recession Analysis*. Alexandria, VA: U.S. Geological Survey, http://pubs.usgs.gov/sir/2005/5160/PDF/Part2_2.pdf (Accessed October 12, 2012).
- Doney, S.C., Lindsay, K., Fung, I., John, J., 2006. Natural Variability in a Stable, 1000-Yr Global Coupled Climate-Carbon Cycle Simulation. *Journal of Climate*, 19: 3033-3054.
- Ek, D., 2004. *Hydrologic and Geochemical Cycling within Karst Versus Non-Karst Basins Within the Interior Low Plateau Province of South-Central Kentucky*. M.S. Thesis, Department of Geography and Geology, Western Kentucky University, Bowling Green, KY.
- EPA (Environmental Protection Agency), 2013. Carbonate, Bicarbonate and Total Alkalinity: Standard Methods 2320 (Titration Method). Washington, D.C.: EPA. Online at: <http://www.epa.gov/region9/qa/pdfs/2320dqi.pdf> (Accessed October 23, 2013).
- EPA (Environmental Protection Agency), 2012. *Environmental Technology Verification Protocol, Drinking Water Systems Center: Generic Protocol for the Product Specific Challenge Testing of Bag and Cartridge Filter Systems*. Washington, D.C.: EPA. Online at: http://www.epa.gov/etv/pubs/01_vp_drt.pdf (Accessed January 25, 2014).
- EPA (Environmental Protection Agency), 2007. *Method 9056: Determination of Inorganic Anions by Ion Chromatography*. Washington, D.C.: EPA. Online at: <http://www.epa.gov/osw/hazard/testmethods/sw846/pdfs/9056a.pdf> (Accessed January 9, 2014).
- Falkowski, P., Scholes, R.J., Boyle, E., Canadell, J., Canfield, D., Elser, J., Gruber, N., Hibbard, K., Högberg, P., Linder, S., Mackenzie, F.T., Moore III, B., Pedersen, T., Rosenthal, Y., Seitzlinger, S., Smetacek, V., Steffen, W., 2000. The Global Carbon Cycle: A Test of Our Knowledge of Earth as a System. *Science*, 290: 291-296.

- Fondriest Environmental, 2006. *Calibration of YSI Sensors*. Online at: <http://www.fondriest.com/pdf/Calibration.pdf> (Accessed July 12, 2013).
- Friedlingstein, P., Cox, P., Betts, R., Bopp, L., Bloh, W. Von, Brovkin, V., Cadule, P., Doney, S., Eby, M., Fung, I., Bala, G., John, J., Jones, C., Joos, F., Kato, T., Kawamiya, M., Knorr, W., Lindsay, K., Matthews, H. D., Raddatz, T., Rayner, P., Reick, C., Roeckner, E., Schnitzler, K.-G., Schnur, R., Strassmann, K., Weaver, A.J., Yoshikawa, C., Zeng, N., 2006. Climate-Carbon Cycle Feedback Analysis: Results from the C⁴MIP Model Intercomparison. *Journal of Climate*, 19: 3337-3353.
- Grabowski Jr., G.J., 2001. *Mississippian System*. Alexandria, VA: U.S. Geological Survey. Online at: <http://pubs.usgs.gov/pp/p1151h/miss.html> (Accessed December 15, 2012).
- Groves, C., Meiman, J., 2005. Weathering, Geomorphic Work, and Karst Landscape Evolution in the Cave City Groundwater Basin, Mammoth Cave, Kentucky. *Geomorphology*, 67.1: 115- 126.
- Groves, C., Meiman, J., 2002. *Strong Acids and the Carbonate Mineral Weathering Atmospheric Carbon Sink*. Geological Society of America Programs with Abstracts, Abstract 98-12, Denver. Colorado, October 28.
- Groves, C., Meiman J., 2001. *Inorganic Carbon Flux and Aquifer Evolution in the South Central Kentucky Karst*. U.S. Geological Survey Karst Interest Group Proceedings, Water-Resources Investigations Report 01-4011: 99-105.
- Groves, C., Meiman, J., Despain, J., Liu, Z., Yuan, D., 2002. *Karst Aquifers as Atmospheric Carbon Sinks: an Evolving Global Network of Research Sites*. U.S. Geological Survey Water-Resources Investigations Report 02-4174: 32-39.
- Harned, H.S, Owen, B.B., 1958. *The Physical Chemistry of Electrolyte Solution*. New York, NY: Reinhold.
- Hatcher, B. E., 2013. *Sources of CO₂ Controlling the Carbonate Chemistry of the Logsdon River, Mammoth Cave, Kentucky*. M.S. Thesis, Department of Geography and Geology, Western Kentucky University, Bowling Green, KY.
- He, S., Kang, S., Li, Q., Wang, L., 2012. The Utilization of Real-Time High Resolution Monitoring Techniques in Karst Carbon Sequestration: A Case Study of the Station in Banzhai Subterranean Stream Catchment. *Advances In Climate Change Research*, 3(1): 54-58.
- Hollander, D. J., McKenzie, J. A., 1991. CO₂ Control on Carbon-Isotope Fractionation During Aqueous Photosynthesis: A Paleo-pCO₂ Barometer. *Geology*, 19: 929-932.

- Jackson, P.E., 2000. Ion Chromatography in Environmental Analysis. In Meyers, R.A. (ed.) *Encyclopedia of Analytical Chemistry*. Chichester, U.K.: John Wiley and Sons, 2779-2801.
- Joos, F., Gerber, S., Prentice, I.C., Otto-Bliesner, B.L., Valdes, P.J., 2004. Transient Simulations of Holocene Atmospheric Carbon Dioxide and Terrestrial Carbon Since the Last Glacial Maximum. *Global Biogeochemical Cycles*, 18: 1-18.
- Katz, B.G., DeHan, R.S., Hirten, J.J., Catches, J.S., 1997. Interactions Between Ground Water and Surface Water in the Suwannee River Basin, Florida. *Journal of the American Water Resources Association*, 33 (6): 1237-1254.
- KGS (Kentucky Geological Survey), 2013. *KY Springs, KY Sinkholes, KYGS_Geology_24K*. Online at: [arctgis on kgs.uky.edu](http://arctgis.kgs.uky.edu) (Accessed January 2013- June 2014).
- KGS (Kentucky Geological Survey), 2012. *Kentucky Geologic Map Information Service*. Online at: <http://kgs.uky.edu/kgsmap/kgsgeoserver/viewer.asp> (Accessed November 12, 2012).
- KGS (Kentucky Geological Survey), 1939. *Mississippian*. Online at: <http://www.uky.edu/OtherOrgs/KPS/goky/pages/gokych06.htm> (Accessed December 15, 2012).
- Lee, E.S., Krothe, N.C., 2001. A Four-Component Mixing Model for Water in a Karst Terrain in South-Central Indiana, USA, Using Solute Concentration and Stable Isotopes as Tracers. *Chemical Geology*, (179): 129-143.3
- Liu, Z., Zhao, J., 2000. Contribution of Carbonate Rock Weathering to the Atmospheric CO₂ Sink. *Environmental Geology*, 39: 1053-1058.
- Liu, Z., Dreybrodt, W., Wang, H., 2010. A New Direction in Effective Accounting for the Atmospheric CO₂ Budget: Considering the Combined Action of Carbonate Dissolution, the Global Water Cycle and Photosynthetic Uptake of DIC by Aquatic Organisms. *Earth-Science Reviews*, 99: 162-172.
- Liu, Z., Dreybrodt, W., Wang, H., 2008. A Possible Important CO₂ Sink by the Global Water Cycle. *Chinese Science Bulletin*, 53(3): 402-407.
- Liu, Z., Groves, C., Yuan, D., Meiman, J., Jiang, G., He, S., Li, Q., 2004. Hydrochemical Variations During Flood Pulses in the South-West China Peak Cluster Karst: Impacts of CaCO₃-H₂O-CO₂ Interactions. *Hydrological Processes*, 18(13): 2423-2437.
- Long, S.E., Martin, T.D., Martin, E.R., Creed, J.T., Brockhoff, C.A., 1994. Method 200.8: Determination of Trace Elements in Waters and Wastes by Inductively Coupled Plasma- Mass Spectrometry: Revision 5.4 EMMC Version. Washington. D.C.: EPA.

- Ludwig, W., Amiotte-Suchet, P., Probst, J. L., 1999. Enhanced Chemical Weathering of Rocks During The Last Glacial Maximum: A Sink For Atmospheric CO₂? *Chemical Geology*, 159 (1): 147-161.
- Lüthi, D., Le Floch, M., Bereiter, B., Blunier, T., Barnola, J.M., Siegenthaler, U., Raynaud, D., Jouzel, J., Fischer, H., Kawamura, K., Stocker, T.F., 2008. High-Resolution Carbon Dioxide Concentration Record 650,000–800,000 Years Before Present. *Nature*, 453(7193): 379-382.
- Master, L.L., Flack, S.R., Stein, B.A. (eds.), 1998. *Rivers Of Life: Critical Watersheds for Protecting Freshwater Biodiversity*. Arlington, VA: The Nature Conservancy.
- McFarlan, A.C., 1943. *Geology of Kentucky*. Baltimore, MD, Waverly Press, Inc.
- Mehnert, E., Dey, W.S., Hwang, H., Keefer, D.A., Holm, T.R., Johnson, T.M., Beaumont, W.C., Wander, M.C.F., Sanford, R.A., McDonald, J.M., Shiffer, S.M., 2005. *Mass Balance of Nitrogen and Phosphorus in an Agricultural Watershed: the Shallow Groundwater Component*. Champaign, IL: Illinois State Geological Survey, Open-File Series Report 2005-3.
- Meybeck, M., 1983. *Atmospheric Inputs and River Transport of Dissolved Substances, Dissolved Loads of Rivers and Surface Water Quantity/Quality Relationships*. Proceedings of the Hamburg Symposium, IAHS (141), August.
- Montety, V. de, Martin, J.B., Cohen, M.J., Foster, C., Kurz, M.J., 2010. Influence Of Diel Biogeochemical Cycles on Carbonate Equilibrium. *Chemical Geology*, 283: 31-43.
- Moore, P J., Martin, J.B., Sreaton, E.J., 2009. Geochemical and Statistical Evidence of Recharge, Mixing, and Controls on Spring Discharge in an Eogenetic Karst Aquifer. *Journal of Hydrology*, 376: 443-455.
- Murray, K., Wade, P. 1996. Checking anion-cation charge balance of water quality analyses: Limitations of the traditional method for non-potable waters. *Water SA*, 22(1): 27-32
- O'Driscoll, M.A., DeWalle, D.R., 2006. Stream-Air Temperature Relations to Classify Stream-Ground Water Interactions in a Karst Setting, Central Pennsylvania, USA. *Journal of Hydrology*, 329: 140-153.
- Palmer, A., 2007. *Cave Geology*. Dayton, OH, Cave Books.
- Perrin, A.S., Probst, A., Probst, J.L., 2008. Impact of Nitrogenous Fertilizers on Carbonate Dissolution in Small Agricultural Catchments: Implications for Weathering CO₂ Uptake at Regional and Global Scales. *Geochimica et Cosmochimica Acta*, 72 (13): 3105-3123.
- Raymond, P.A., Caraco, N.F., Cole, J.J., 1997. Carbon Dioxide Concentration and Atmospheric Flux in the Hudson River. *Estuaries*, 20.2: 381-390.

- Sarmiento, J.L., Sundquist, E.T., 1992. Revised Budget for the Oceanic Uptake of Anthropogenic Carbon Dioxide. *Nature*, 356: 589-593.
- Schackleton, N.J., 2000. The 100,000- Year Ice-Age Cycle Identified and Found to Lag Temperature, Carbon Dioxide, and Orbital Eccentricity. *Science*, 289: 1897-1902.
- Siegenthaler, U., Sarmiento, J.L., 1993. Atmospheric Carbon Dioxide and the Ocean. *Nature*, 365: 119-125.
- Sigman, D.M., Boyle, E.A., 2000. Glacial/Interglacial Variations in Atmospheric Carbon Dioxide. *Nature*, 407: 859-869.
- Stumm, W., Morgan, J.J., 1996. *Aquatic chemistry: Chemical Equilibria and Rates in Natural Waters*: Vol. 126. Danvers, MA: John Wiley & Sons.
- Sundquist, E.T., 1993. The global carbon dioxide budget. *Science*, 259(5097): 934-941.
- Twenhofel, W.H., 1931. *The Building of Kentucky*. Lexington, KY: The Kentucky Geological Survey.
- USDA (United States Department of Agriculture), 2013. *Natural Resources Conservation Service*. Washington, D.C.: USDA. Online at: <http://www.nrcs.usda.gov/wps/portal/nrcs/site/national/home/>
- Waters (Water Analysis Training Education and Research Services), 2009. *Analyses: Ion Delective Electrode (ISE)*. Online at: <http://waters.waterky.org/node/8832#Misc> (Accessed January 9, 2014).
- White, W.B., 2013. Carbon fluxes in Karst aquifers: Sources, Sinks, and the Effect of Storm Flow. *Acta Carsologica*, 42: 2-3.
- White W.B., White E.L., 1989. *Karst Hydrology Concepts from the Mammoth Cave Area*. New York, NY, Van Nostrand Reinhold.
- Williams P.W., Fong, Y.T., 2010. *Karst Regions of the World*. Circle of Blue online at: <http://www.circleofblue.org/waternews/wp-content/uploads/2010/01/world-karst-map-web-1.12.jpg>, (Accessed March 29, 2013).
- Worthington, S.R.H., 2003. A Comprehensive Strategy For Understanding Flow in Carbonate Aquifer: Speleogenesis and Evolution of Karst Aquifers. *The Virtual Scientific Journal*, 1(1): 1-8.
- Yuan, D., 1988. *On The Karst Environmental System*. In IAH 21st Congress on Karst Hydrogeology And Karst Environment Protection, Institute of Karst Geology, Guilin, Guangxi, China, 30-46.

